



This is a repository copy of *Modelling, simulation, thermodynamic and economic performance analysis of steam and CO<sub>2</sub> as diluents in thermal cracking furnace for ethylene manufacturing*.

White Rose Research Online URL for this paper:

<https://eprints.whiterose.ac.uk/221094/>

Version: Accepted Version

---

**Article:**

Zhang, Y., Yan, H., Chong, D. et al. (4 more authors) (2025) Modelling, simulation, thermodynamic and economic performance analysis of steam and CO<sub>2</sub> as diluents in thermal cracking furnace for ethylene manufacturing. *Fuel*, 381 (Part D). 133656. ISSN 0016-2361

<https://doi.org/10.1016/j.fuel.2024.133656>

---

© 2024 The Authors. Except as otherwise noted, this author-accepted version of a journal article published in *Fuel* is made available via the University of Sheffield Research Publications and Copyright Policy under the terms of the Creative Commons Attribution 4.0 International License (CC-BY 4.0), which permits unrestricted use, distribution and reproduction in any medium, provided the original work is properly cited. To view a copy of this licence, visit <http://creativecommons.org/licenses/by/4.0/>

**Reuse**

This article is distributed under the terms of the Creative Commons Attribution (CC BY) licence. This licence allows you to distribute, remix, tweak, and build upon the work, even commercially, as long as you credit the authors for the original work. More information and the full terms of the licence here:

<https://creativecommons.org/licenses/>

**Takedown**

If you consider content in White Rose Research Online to be in breach of UK law, please notify us by emailing [eprints@whiterose.ac.uk](mailto:eprints@whiterose.ac.uk) including the URL of the record and the reason for the withdrawal request.



[eprints@whiterose.ac.uk](mailto:eprints@whiterose.ac.uk)  
<https://eprints.whiterose.ac.uk/>

# Modelling, simulation, thermodynamic and economic performance analysis of steam and CO<sub>2</sub> as diluents in thermal cracking furnace for ethylene manufacturing

Yao Zhang <sup>a</sup>, Hui Yan <sup>b,a</sup>, Daotong Chong <sup>b</sup>, Cailing Guo<sup>b</sup>, Shengyuan Huang<sup>a</sup>, Joan Cordiner<sup>a</sup> and  
\*Meihong Wang <sup>a</sup>

<sup>a</sup> *Department of Chemical and Biological Engineering, The University of Sheffield, Sheffield S1 3JD, UK*

<sup>b</sup> *State Key Laboratory of Multiphase Flow in Power Engineering, Xi'an Jiaotong University, Xi'an, Shaanxi, China*

\*Corresponding author: Tel.: +44 (0) 114-222-7160. E-mail: Meihong.Wang@sheffield.ac.uk

## Abstract

Energy consumption, economic and environmental benefits of thermal cracking furnace have been important topics in ethylene manufacturing. Use of captured CO<sub>2</sub> as alternative diluent in thermal cracking furnace can significantly contribute to CO<sub>2</sub> reduction while the studies on CO<sub>2</sub> as diluent are limited and inaccurate. To carry out comparative analysis of using steam and CO<sub>2</sub> as diluents in propane cracking for ethylene manufacturing, a 1-dimensional (1-D) pseudo-dynamic model of plug flow reactor (PFR) was developed and implemented in gPROMS ModelBuilder<sup>®</sup>. The model was validated and showed good agreement with industrial data from literature and then was used to analyse the economic and thermodynamic performance of PFR using different diluents. The process analysis includes: (1) impact of diluent-to-propane ratio using steam as diluent; (2) impact of diluent-to-propane ratio using CO<sub>2</sub> and compared with using steam; (3) comparison of pure/mixed diluents in 4 different scenarios. The results indicated that the PFR could reach highest annual production at the steam-to-propane ratio 0.2 and reach highest annual profit at the ratio 0.3 when using steam as diluent. Compared with steam, using CO<sub>2</sub> as diluent hardly changes the annual production, but can significantly increase the run length and the annual profit. The highest annual profit using CO<sub>2</sub> is 10.10% higher than that using steam and when operating

1 at the diluent-to-propane ratio achieving highest annual profit, using CO<sub>2</sub> as diluent can save 17.44%  
2 energy and reduce the exergy destruction by 20.53%. Pure CO<sub>2</sub> was recommended as diluent from  
3 comparison of pure/mixed diluents in 4 different scenarios. The key findings of this paper provide  
4 significant operational guidance for existing thermal cracking furnace using steam as diluent and also  
5 provide insights for future new generation diluents design to reduce the energy consumption in quantity  
6 and quality and increase the economic benefits of thermal cracking furnace for ethylene manufacturing.

7 Keywords: Ethylene manufacturing; Thermal cracking furnace; Diluents; Modelling and simulation;  
8 Economic analysis, Energy and exergy analysis.

## 1 **Abbreviations**

2 1-D, 1-dimensional;

3 3-D, 3-dimensional;

4 COT, Coil outlet temperature;

5 PFR, Plug flow reactor.

## 6 **Nomenclature**

7	$A_c$	Pre-exponential factor for coking reaction [ $\text{kg m}^3/(\text{kmol m}^2 \text{ s})$ ]
8	$A_j$	Pre-exponential factor for reaction j [ $\text{s}^{-1}$ ] or [ $\text{m}^3/(\text{kmol s})$ ]
9	$C_i(z)$	Molar concentration of component i [ $\text{kmol/m}^3$ ]
10	$COS_{\text{annual}}$	Annual cost [\$/year]
11	$COS_{\text{diluent}}$	Price factor of diluent [\$/kg]
12	$COS_{\text{heat}}$	Price factor of heat [\$/kg]
13	$COS_i$	Price factor of component i [\$/kg]
14	$Cpm_d$	Specific heat capacity of diluent [ $\text{kJ}/(\text{kg K})$ ]
15	$Cpm_i(z)$	Specific heat capacity of component i [ $\text{kJ}/(\text{kg K})$ ]
16	$D(z)$	Internal diameter of PFR with coke formation [m]
17	$DCC$	Decoking cost per cycle [\\$]
18	$D_i$	Internal diameter of PFR under clean tube condition [m]
19	$Dt$	External diameter of PFR [m]
20	$Ea_j$	Activation energy of reaction j [ $\text{kJ}/\text{kmol}$ ]
21	$E_c$	Activation energy of coking reaction [ $\text{kJ}/\text{kmol}$ ]
22	$\dot{E}^{ch}$	Chemical exergy [ $\text{kJ}/\text{s}$ ]
23	$\dot{E}^{ph}$	Physical exergy [ $\text{kJ}/\text{s}$ ]
24	$\dot{E}_D$	Exergy destruction of PFR [ $\text{kJ}/\text{s}$ ]
25	$\dot{E}_{D,\text{annual}}$	Annual exergy destruction of PFR [ $\text{GJ}/\text{year}$ ]

1	$\dot{E}_{D,ht}$	Exergy destruction caused by heat transfer [kJ/s]
2	$\dot{E}_{D,re}$	Exergy destruction caused by chemical reactions [kJ/s]
3	$\dot{E}_{D,total}$	Exergy destruction of PFR in a cycle of run length [GJ]
4	$\dot{E}_{f,in}$	Exergy of PFR inlet stream [kJ/s]
5	$\dot{E}_{f,out}$	Exergy of PFR outlet stream [kJ/s]
6	$\dot{E}_i^0$	Molar standard chemical exergy of component i [kJ]
7	$\dot{E}_k^0$	Molar standard chemical exergy of element k [kJ]
8	$\dot{E}_Q$	Exergy of required heat [kJ/s]
9	$\dot{E}_{Q,annual}$	Annual exergy of required heat [GJ/year]
10	$\dot{E}_{Q,total}$	Exergy of required heat in a cycle of run length [GJ]
11	$F_d(z)$	Mass flowrate of diluent [kg/s]
12	$F_i(z)$	Mass flowrate of component i [kg/s]
13	$F_{i\ annual}$	Annual production of component i [kg/year]
14	$F_{i\ total}$	Total production of component i in a cycle of run length [kg]
15	$Fr(z)$	Friction factor [ $m^{-1}$ ]
16	$G(z)$	Total mass flow rate [ $kg/m^2\ s$ ]
17	$h_g(z)$	Heat transfer coefficient of process gas [ $W/(m^2 \cdot K)$ ]
18	$H$	Enthalpy of the stream [kJ/s]
19	$INC_{annual}$	Annual income [\$/year]
20	$L$	Reactor length [m]
21	$MW_i$	Molecular weight of component i [kg/kmol]
22	$N_{diluent}$	Molar flowrate of diluent [kmol/s]
23	$NC$	Number of components [-]
24	$NR$	Number of reactions [-]
25	$NE$	Number of elements [-]
26	$n_{ij}$	Reaction order [-]

1	$n_{i,k}$	Number of element k in component i [-]
2	$P(z)$	Pressure [Pa]
3	$P_0$	Pressure of reference environmental state
4	$P_{\text{annual}}$	Annual profit [\$/year]
5	$\dot{Q}(z)$	Heat transfer rate [kJ/s]
6	$\dot{Q}_{\text{annual}}$	Annual energy consumption [GJ/year]
7	$\dot{Q}_{\text{total}}$	Total energy consumption in a cycle of run length [GJ]
8	$R$	Ideal gas constant [J/ (K mol)]
9	$R_1(z)$	Thermal resistivity relative to gas convection [K/kW]
10	$R_2(z)$	Thermal resistivity relative to coke conductivity [K/kW]
11	$R_3(z)$	Thermal resistivity relative to tube conductivity [K/kW]
12	$r_c(z)$	Reaction rate of coking [g / (m <sup>2</sup> s)]
13	$r_j(z)$	Reaction rate of reaction j [kmol/ (s m <sup>3</sup> )]
14	$s_{ij}$	Stoichiometry coefficient [-]
15	$S$	Entropy of the stream [kJ/ (s K)]
16	$T_0$	Temperature of reference environmental state
17	$T(z)$	Process gas temperature [K]
18	$T_c(z)$	Coke surface temperature [K]
19	$T_{we}(z)$	Tube outer wall temperature [K]
20	$T_{wi}(z)$	Tube inner wall temperature [K]
21	$t_c$	Run length [hr]
22	$t_d$	Decoking time per cycle [hr]
23	$x(z)$	Global composition of stream [-]
24	$x_i(z)$	Mole fraction of component i [-]
25	<b>Greek letters</b>	
26	$\Delta G_f^0$	Standard Gibbs energy of formation [J/mol]
27	$\Delta H_{r,j}(z)$	Heat of reaction [kJ/kmol]

1	$\lambda_c$	Conduction heat transfer coefficient of coke [kJ/(s m K)]
2	$\lambda_t(z)$	Conduction heat transfer coefficient of tube wall [kJ/(s m K)]
3	$\delta(z)$	Coke thickness [m]
4	$\varphi_c$	Coke density [kg/m <sup>3</sup> ]
5	$\varepsilon$	Rational exergy efficiency [-]
6	$\varepsilon_{annual}$	Annual average rational exergy efficiency [-]
7		

## 1. Introduction

Thermal cracking of hydrocarbon in a thermal cracking furnace is the main technology to produce ethylene and propylene, which are the basic raw materials of petrochemical industry [1]. As the core equipment in ethylene manufacturing, thermal cracking furnace (shown in **Fig. 1**) directly determines different key aspects including production capacity, economic benefits, energy consumption and CO<sub>2</sub> emission of ethylene manufacturing [2,3].

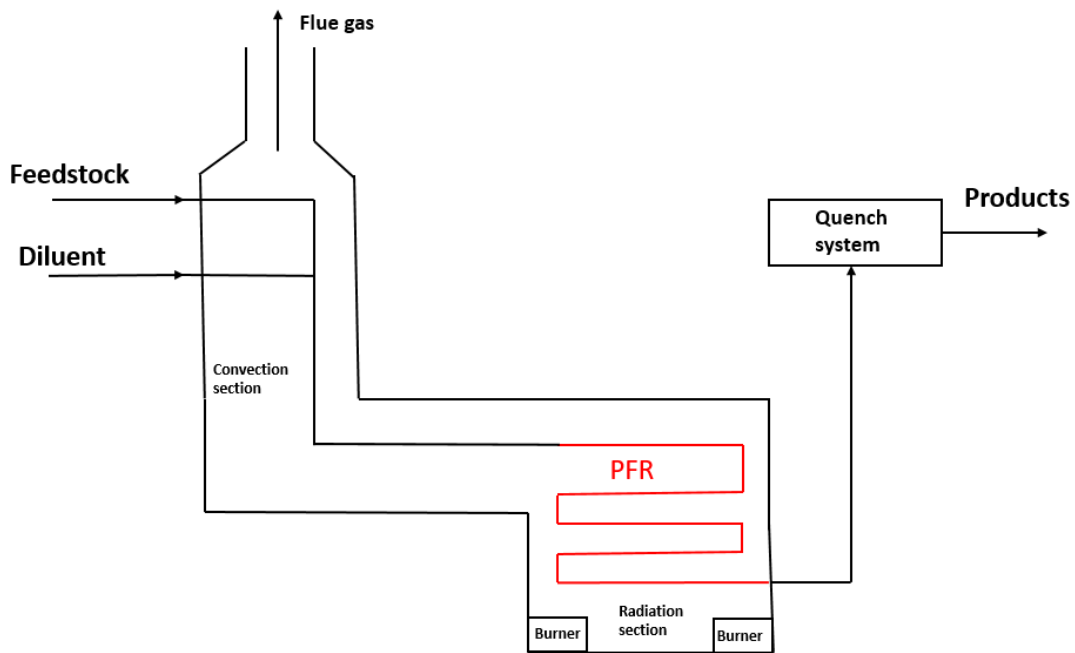


**Fig. 1.** Schematic diagram of a typical thermal cracking furnace [4]

Most existing studies [5-8] of thermal cracking furnace focus on the plug flow reactor (PFR) in radiation section since the PFR has the most significant impact on the final products of the thermal cracking furnace. The burners in radiation section provide heat to the PFR to maintain the required temperature profile for cracking reactions to take place [9]. In convection section, the feedstock and diluent are mixed and preheated. The process gas reaches the temperature for cracking when it leaves the convection section. In quench system, the temperature of cracked process gas from PFR is reduced rapidly to inhibit the undesired reactions [10].

The primary function of the diluent is to reduce undesired secondary reaction rates and the coking rate by lowering the hydrocarbon partial pressure. This function can be explained by Law of Mass Action,

1 which states that, at a given temperature, the reaction rate is directly proportional to the product of the  
2 concentrations (partial pressure in gas phase system) of the reactants. However, the primary reaction  
3 rate is also reduced for the same reason which will reduce the conversion rate of feedstock. Therefore, it  
4 is important to study the impact of diluent-to-feedstock ratio on the performance of PFR in thermal  
5 cracking furnace through modelling and simulation. Steam is the most commonly used diluent in thermal  
6 cracking process for ethylene manufacturing. Only two studies explored the potential of using CO<sub>2</sub> as  
7 diluent [11, 12]. Carbon dioxide can serve as a diluent because, like steam, it exists in the gaseous phase  
8 at high temperatures and has thermal stability and chemical inertness. However, the differing physical  
9 properties of these two diluents, including molecular weight, specific heat capacity, and vapor thermal  
10 conductivity, lead to variations in the thermodynamic and economic performance of the PFR. Hu et al.  
11 [13] investigated the huge potential of applying carbon capture process for ethylene manufacturing.  
12 However, the cost of CO<sub>2</sub> transport and storage is extremely high [14]. Utilizing captured CO<sub>2</sub> as  
13 alternative diluent in ethylene manufacturing process is preferred since it can avoid the extra cost of CO<sub>2</sub>  
14 transport and storage.

15 In modelling and simulation work, a reaction scheme is a detailed representation of the chemical reactions  
16 taking place within the PFR. Layokun and Slater [16] developed a reaction scheme including 19 free-  
17 radical reactions for pyrolysis of propane between 600 and 800 °C. To represent the complex free-radical  
18 reactions of propane cracking and to reduce the computational demand, reaction scheme based on  
19 molecular reaction mechanism developed by Sundaram and Froment [17] has been widely used in  
20 existing literature. However, this reaction scheme did not consider the coke formation on the tube inner  
21 wall of PFR. Therefore, Sundaram and Froment [15] improved the previous reaction scheme through  
22 adding 2 molecular reactions of coke formation.

23 In recent years, several studies have focused on modelling and simulation of PFR to improve energy  
24 efficiency and profitability. Shahrokhi and Nejati [6] developed a 1-dimensional (1-D) steady-state model  
25 of PFR for propane cracking. This model was used to find out the optimal process gas temperature profile  
26 to obtain the maximum operating profit. Although the effects of decoking time and cost of decoking  
27 process was considered, the coking rate used was not accurate since it was assumed not change with

1 time. Gao et al. [5] carried out a steady-state simulation of the PFR for naphtha cracking using Aspen  
2 HYSYS®. The effects of process gas temperature profile and steam-to-naphtha ratio on valuable product  
3 yields and steady-state coking rate were analysed. Berreni and Wang [8] developed a 1-D pseudo-  
4 dynamic model of PFR for propane cracking considering the coke formation dynamically. This model was  
5 implemented in gPROMS ModelBuilder® and the simulation results were used to analyse (a) effects of  
6 different process gas temperature profiles on valuable products yields and production time and (b) coke  
7 formation on heat transfer, valuable products yields and production time.

8 As for the steam as diluent, several experimental and simulation studies have examined the influence of  
9 steam-to-feedstock ratios on the performance of thermal cracking process. Keyvanloo et al. [18] did  
10 experiments of naphtha cracking to study the effects of different steam-to-naphtha ratios on the yields of  
11 olefins at lab scale. Their experimental results indicated that a higher steam-to-naphtha ratio could  
12 increase the yields of ethylene without considering the coke formation. Gao et al. [5] analysed the impact  
13 of steam-to-naphtha ratio on yields of valuable products and coking rate under clean tube condition  
14 through steady-state simulation. The results indicated that higher steam-to-naphtha ratio could increase  
15 the ethylene yield and decrease the coking rate while the impact on propylene yield was tiny.

16 However, research on the use of CO<sub>2</sub> as a diluent is currently limited, with only two studies exploring its  
17 potential [11, 12]. Yancheshmeh et al. [11] compared the impact of using steam as diluent and using CO<sub>2</sub>  
18 as diluent in ethane thermal cracking through dynamic modelling and simulation. Their simulation results  
19 indicated that using CO<sub>2</sub> as diluent can improve the productions of ethylene and hydrogen and increase  
20 the run length of the PFR when the diluent-to-ethane ratio was fixed at 2kg diluent/1kg ethane. However,  
21 their model did not study heat transfer carefully, assuming no temperature difference along radial  
22 direction from tube outer wall to process gas. In addition, their simulation result of COT has 30K  
23 differences compared with the industrial data. These two limitations significantly reduced the accuracy  
24 and reliability of their simulation results since the reactions of both thermal cracking and coke formation  
25 are extremely temperature sensitive. Haghighi et al. [12] compared the two kinds of diluents using  
26 naphtha as feedstock. Their study has the same two limitations as the study of Yancheshmeh et al. [11].  
27 Research on the use of CO<sub>2</sub> as a diluent lacks comparison of various diluent-to-feedstock ratios with

1 steam. Additionally, a comprehensive comparison of thermodynamic performance and economic benefits  
2 is necessary.

3 Ethylene manufacturing is one of the most energy demanding industries [2]. As a tool based on second  
4 law of thermodynamics to analysis the quality of energy, it is necessary to implement exergy analysis in  
5 the ethylene manufacturing [19]. Alizadeh et al. [20] carried out conventional exergy analysis through  
6 hybrid modelling of thermal cracking furnace in ethylene manufacturing. The exergy efficiency of each  
7 unit in thermal cracking furnace and the source of exergy destruction were determined in this study. Yuan  
8 et al. [4] carried out conventional and advanced exergy analysis of thermal cracking furnace to find out  
9 the energy saving potential. The results of their study indicated that the PFR in radiation section has huge  
10 avoidable exergy destruction, most of the avoidable exergy destruction is caused by the PFR itself.  
11 Therefore, it is urgent to study the PFR for energy saving. Shen et al. [21] analysed the exergy efficiency  
12 of down-stream separation process in ethylene manufacturing. In addition, a Pareto frontier has been  
13 found to maximum the exergy efficiency of the system with lowest operational cost through multi-objective  
14 optimisation.

15 No study carried out exergy analysis focusing on the PFR in radiation section of thermal cracking furnace.  
16 However, few studies carried out exergy analysis of the similar reactors in other processes. Aghbashlo  
17 et al. [22] carried out exergy, economic and environmental assessment of the tubular reactor for ethanol  
18 dehydration to diethyl ether. Zhang et al. [23] considered the reactor for methanol decomposition as PFR  
19 and carried out energy and exergy analysis of the reactor using solar energy. Their study indicated that  
20 the exergy destruction in this process is mainly caused by chemical reactions and solar concentrating.  
21 Choe et al. [24] simulated the steam reforming unit as tubular reactor for carbon capture and liquefaction  
22 using Aspen HYSYS<sup>®</sup>. Then energy, exergy, economic and environmental analysis were carried out on  
23 the system to compare 4 cases.

24 This paper aims to carry out a comparative analysis of using different diluents (e.g. steam vs CO<sub>2</sub>) for  
25 their thermodynamic and economic performance in propane cracking for ethylene manufacturing through  
26 modelling and simulation. In comparison with previous studies, this paper has the following novel  
27 contributions:

1 (a) It is the first study that dynamically analyses the impact of different diluent-to-propane ratios on  
2 ethylene manufacturing using steam as diluent.

3 In existing literatures, only Gao et al. [5] and Keyvanloo et al. [18] studied the impact of different steam-  
4 to-feedstock ratios on the PFR performance at steady state (under clean tube condition only). However,  
5 due to the dynamic growth of coke layers, a study considering the entire run length is necessary. This  
6 study will fill the research gap through pseudo-dynamic modelling, simulation, and analysis.

7 (b) It is the first study that dynamically analyses the impact of different diluent-to-propane ratios on  
8 ethylene manufacturing using CO<sub>2</sub> as diluent and carries out comparative analysis with steam for  
9 their economic and thermodynamic performance.

10 Although two previous studies explored the potential of using CO<sub>2</sub> as diluent in ethylene manufacturing  
11 [11, 12], the analysis of using this diluent remains limited. Neither study considered the temperature  
12 gradient from the tube outer wall to the process gas, leading to inaccurate simulation results. In addition,  
13 these two existing studies compared CO<sub>2</sub> with steam as diluent at only one diluent-to-feedstock ratio for  
14 the production capacity of valuable products. A research gap was identified concerning the analysis of  
15 varying diluent-to-feedstock ratios and the comprehensive evaluation of thermodynamic performance  
16 and economic benefits. In this study, a more accurate pseudo-dynamic model of the PFR will be  
17 developed to carry out comparative analysis of using CO<sub>2</sub> as diluent with steam at different diluent-to-  
18 propane ratios considering profits and consumption of energy in quantity and quality.

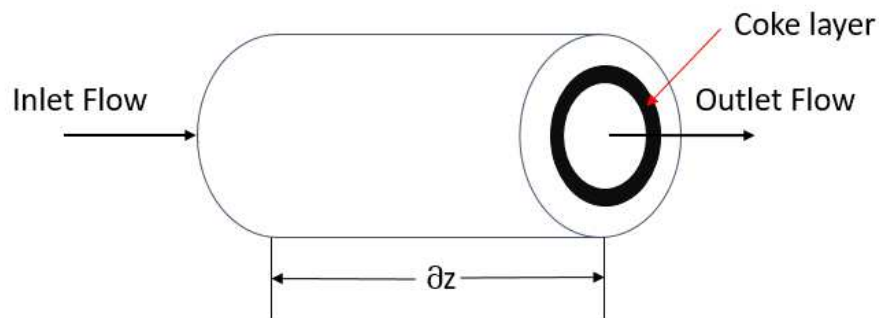
19 (c) It is the first study that proposes the possibility of using mixed diluent and compares four different  
20 scenarios in ethylene manufacturing.

21 No previous study explored the possibility of using mixed diluent in existing literature. In this study, four  
22 different scenarios using different diluents at different diluent-to-propane ratios will be studied. The key  
23 performance indicators of economic performance including run length, annual production of valuable  
24 products and annual profit and thermodynamic performance including annual exergy destruction and  
25 annual average exergy efficiency will be compared.

## 1 2. Mathematic modelling

### 2 2.1 Process description

3 In this study, propane is chosen as the feedstock. A schematic of the PFR front view is shown in Fig. 2,  
4 the inlet flow is the process gas consisting of a mixture of propane and diluent from convection section.  
5 The outlet flow shown in Fig. 2 is process gas consisting of products after thermal cracking. These  
6 products will be sent to the quench system to inhibit over-cracking. The coke layer is formed on the tube  
7 inner wall because of the undesired coking reactions. The coke layer will reduce the PFR volume and  
8 increase the total thermal resistance from the tube outer wall to the process gas.



9  
10 **Fig. 2.** Schematic diagram of the PFR front view [8]

11 To maintain the high process gas temperature required by thermal cracking reactions, the PFR tube outer  
12 wall is heated by the burners in radiation section. The heat then transfers from the tube outer wall to the  
13 process gas inside the PFR. The heat transfer process can be generally divided into three parts including  
14 heat conduction inside the metal tube, heat conduction inside the coke layer and heat convection from  
15 coke surface to the process gas. Fig. 3 shows the different layers in PFR from cross-section view.

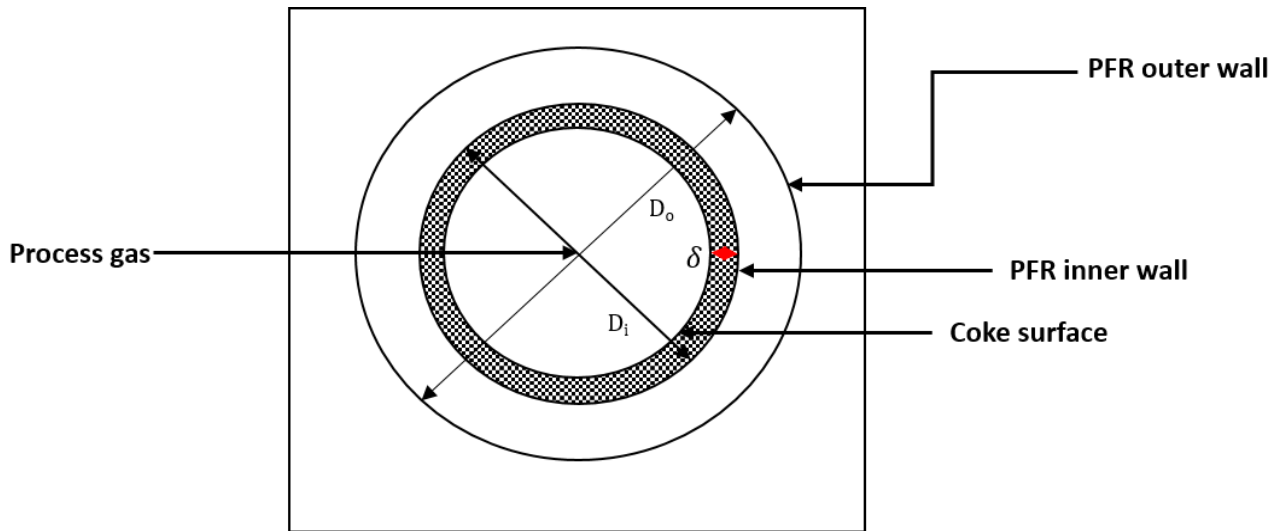


**Fig. 3.** Schematic diagram of the PFR cross-section view [8]

Table 1 shows the reaction scheme developed by Sundaram and Froment in 1979, which is applied in this research to describe the thermal cracking reactions and coke formations inside the PFR.

**Table 1.** Reaction scheme for Propane cracking and coke formation [15]

No.	Reactions	A, s <sup>-1</sup> or *m <sup>3</sup> /(kmol s)	E, kJ /mol
1	$C_3H_8 \Rightarrow C_2H_4 + CH_4$	4.692E+10	211.7
2	$C_3H_8 \rightleftharpoons C_3H_6 + H_2$		
	Forward reaction	5.888E+10	214.6
	Backward reaction	*9.04E+5	95.3
3	$C_3H_8 + C_2H_4 \Rightarrow C_2H_6 + C_3H_6$	*2.536E+13	247.1
4	$2C_3H_6 \Rightarrow 3C_2H_4$	1.514E+11	233.5
5	$2C_3H_6 \Rightarrow 0.5C_6 + 3CH_4$	1.423E+9	190.4
6	$C_3H_6 \rightleftharpoons C_2H_2 + CH_4$		
	Forward reaction	3.794E+11	248.5
	Backward reaction	*2.32E+7	123.7
7	$C_3H_6 + C_2H_6 \Rightarrow C_4H_8 + CH_4$	*5.553E+14	251.1
8	$C_2H_6 \rightleftharpoons C_2H_4 + H_2$		
	Forward reaction	4.652E+13	272.8
	Backward reaction	*9.97E+8	138.0
9	$C_2H_4 + C_2H_2 \Rightarrow C_4H_6$	*1.026E+12	172.6

10	$C_4H_8 \Rightarrow C_6$	6.96E+7	143.6
11	$C_3H_6 \Rightarrow \text{Coke}$	**5.82E+11	308.0

---

\*\*Unit: kg Coke/ (kmol s/m)

## 1 2.2 Assumptions

2 To develop a 1-D pseudo-dynamic model of the PFR in thermal cracking furnace, the following  
3 assumptions were made:

- 4 • Steam and  $CO_2$  are considered as inertness in the PFR.
- 5 • All the components inside the PFR are in gas phase.
- 6 • No temperature and concentration difference inside the PFR along the radial direction for the  
7 process gas.
- 8 • All the thermal cracking reactions only take place inside the PFR.
- 9 • The process gas flow is considered as plug flow.
- 10 • Thermal entrance region effects and hydrodynamics are neglected.
- 11 • The process gas is considered as ideal gas when calculating the component concentrations.
- 12 • The coke formation model is considered as pseudo-dynamic.

13 Regarding assumption 1, Yancheshmeh et al. [11] and Haghghi et al. [12] assumed that  $CO_2$  can remove  
14 coke significantly in their modelling studies. However, this is not correct since several studies [25-28]  
15 have proved that the gasification of coke using  $CO_2$  as agent is several times slower than using steam  
16 as agent under the same condition when the pressure varying from 1-20 bars. The pressure of the PFR  
17 is operated from 3 bars at the inlet and reduce to around 2 bars at the outlet. Under this condition, the  
18 partial removal of coke using  $CO_2$  can be ignored (less than 0.1% in difference of coke thickness). There  
19 is merely no reverse water-gas shift reaction because of extremely short residence time, low  $H_2$ :  $CO_2$   
20 ratio and absence of catalyst. A simulation with reverse water-gas shift reaction using the reaction kinetics  
21 supposed by Karim and Mohindra was carried out [29]. The simulation results indicate that less than  
22 0.01wt%  $CO_2$  has been converted. Therefore,  $CO_2$  is assumed as inertness in the PFR in this study.

1 Since the coking rate is extremely slow compared with the reaction rates of thermal cracking reactions,  
2 only the coke thickness change with time in this pseudo-dynamic model. The change of the concentration  
3 of each component with time can be neglected because the coking rate is very low compared with large  
4 mass flowrate of process gas. Only considering the coke thickness change with time can reduce  
5 computational cost while maintaining model accuracy.

6 In this model, only the temperature difference from the outer tube wall to process gas was considered.  
7 The process gas in the PFR was considered as 1-D plug flow with no temperature and concentration  
8 difference along the radial direction. This assumption will lead to minor loss of accuracy since the process  
9 gas near the tube inner wall (coke surface) has slightly higher temperature and concentration of reaction  
10 products in real-world scenarios [30]. The impact of this assumption will be tiny when the diameter-to-  
11 length ratio of the PFR is small. In addition, the 3-dimensional (3-D) model of PFR in existing literature  
12 all focus on the detailed temperature and products distribution in the PFR under steady-state (clean tube  
13 conditions) because of long simulation time [30-32]. The assumption 3 in this study can reduce the  
14 simulation time when considering the dynamic impact of coke formation in this model and generate results  
15 for different cases.

## 16 2.3 Principles and Equations

### 17 2.3.1 Material balance

18 The material balance only considers the concentration change in axial direction along the PFR, which  
19 can be written as:

$$20 \quad \frac{\partial F_i(z)}{\partial z} = \sum_{j=1}^{NR} s_{ij} \times r_j(z) \times M_{wi} \times \frac{\pi \times D(z)^2}{4} \quad (1)$$

21 The reaction scheme shown in Table 1 can be used to calculate the chemical reaction rates and coking  
22 rate according to the Arrhenius law. All the reactions in this reaction scheme is assumed elementary.

$$23 \quad r_j(z) = A_j \times e^{\frac{-Ea_j}{RT(z)}} \times \prod_{i=1}^{NC} C_i^{n_{ij}}(z) \quad (2)$$

1 The reaction rates of thermal cracking reactions can be calculated from equation (2). Similarly, the coking  
 2 rate can be calculated from equation (3).

$$3 \quad r_c(z) = A_c \times e^{\frac{-E_c}{RT_c(z)}} \times C_{C_3H_6}(z) \quad (3)$$

4 Then the coke thickness can be determined by the following equation with coking rate:

$$5 \quad \frac{d\delta(z)}{dt} = \frac{r_c(z)}{\varphi c} \quad (4)$$

6 The coke formation will cause the diameter reduction of the PFR. So, the inner diameter will be influenced  
 7 by coke thickness shown in the following equation:

$$8 \quad D(z) = Di - 2\delta(z) \quad (5)$$

9 Molar concentration of each component can be calculated based on ideal gas law:

$$10 \quad C_i(z) = \left( \frac{\frac{F_i(z)}{MW_i}}{N_{diluent} + \sum_{i=1}^{NC} \left( \frac{F_i(z)}{MW_i} \right)} \right) \times \frac{P(z)}{R \times T(z)} \times \frac{1}{1000} \quad (6)$$

11

### 12 2.3.2 Energy balance

13 Similar as the mass balance, the energy balance only considers the temperature difference in axial  
 14 direction along the PFR:

$$15 \quad \left( \sum_{i=1}^{NC} F_i(z) \times Cpm_i(z) + F_d(z) \times Cpm_d(z) \right) \times \frac{\partial T(z)}{\partial z} = \frac{\dot{Q}(z)}{L} + \frac{\pi \times D(z)^2}{4} \times \sum_{j=1}^{NR} r_j(z) \times \left( -\Delta H_{r,j}(z) \right) \quad (7)$$

16 The high temperature at the PFR tube outer wall transfers heat to process gas to provide the heat required  
 17 by thermal cracking reactions to take place. The heat transfer rate is related to the three thermal  
 18 resistance items of each layer shown in Fig. 3 and can be calculated by the following:

$$19 \quad Q(z) = \frac{1}{R_1(z) + R_2(z) + R_3(z)} (T_{we}(z) - T(z)) \quad (8)$$

20  $R_1$  is the thermal resistance of fluid process gas, which can be determined by:

$$R_1(z) = \frac{1}{D(z)h_g(z)\pi L} \quad (9)$$

$R_2$  is the thermal resistance of coke layer, which can be determined by:

$$R_2(z) = \frac{\ln\left(\frac{D_i}{D(z)}\right)}{2\pi L\lambda_c} \quad (10)$$

$R_3$  is the thermal resistance of metal tube layer, which can be determined by:

$$R_3(z) = \frac{\ln\left(\frac{D_t}{D_i}\right)}{2\pi L\lambda_t} \quad (11)$$

### 2.3.3 Momentum balance

The pressure drop along the PFR can be calculated by the following momentum balance equation:

$$\frac{\partial P(z)}{\partial z} = \frac{\partial\left(\frac{1}{Mm(z)}\right)/\partial z + \frac{1}{Mm(z)} \times \left(\frac{1}{T(z)} \times \frac{\partial T(z)}{\partial z} + Fr(z)\right)}{\frac{1}{Mm(z)P(z)} - \frac{P(z)}{G(z)^2 RT(z)}} \quad (12)$$

## 2.4 Physical properties and implementation

This 1-D pseudo-dynamic model was implemented in gPROMS ModelBuilder<sup>®</sup>. The model should be implemented in the following operating range which Sundaram and Froment developed their reaction scheme [15].

- Diluent-to-propane ratio 0.2-1.0 kg/kg
- COT from 973.15K to 1143.15K
- Outlet pressure of process gas from  $2.3 \times 10^5$  Pa to  $1.2 \times 10^5$  Pa.

The predication of physical properties used in this model is based on Peng-Robinson equation of state and can be obtained from Multiflash<sup>®</sup>. Peng-Robinson equation of state can accurately predict the volumetric and thermodynamic properties for pure substances and mixtures in the operating range of this

1 model [33-35]. Multiflash<sup>®</sup> can provide an external property package and linked with gPROMS  
2 ModelBuilder<sup>®</sup> as a Foreign Object. These two software are both commercially available.

### 3 3. Model validation

#### 4 3.1 Industrial data for model validation

5 The simulation of the pseudo-dynamic PFR model was based on an industrial reactor reported by  
6 Sundaram and Froment [15]. The configuration parameters and the main operating conditions of an  
7 industrial reactor are given in Table 2 and the process gas temperature profile is given in Fig. 4. These  
8 parameters and variables were assigned in the pseudo-dynamic (as inputs) to generate the results for  
9 validation. Two simulation runs were carried out for validation under clean tube condition ( $t = 0$ ) and 700  
10 hours run length. The reporting interval was set as 36,000 seconds (i.e. 10 hours) to reduce the simulation  
11 time since the change of coke thickness in an hour is indistinguishable.

12 **Table 2.** Parameters of an industrial reactor [15]

Parameters/variable	Value
Length of the coil in the radiant section	95 [m]
Length of the straight portion of the coil	8.85 [m]
Length of the bends	0.553 [m]
Radius of the bends	0.178 [m]
Tube diameter	$\Phi$ 0.116 $\times$ 0.008 [m]
Total feed per coil	0.7635 [kg/s]
Steam dilution rate	0.4 [kg steam/kg propane]
Inlet pressure	$3 \times 10^5$ [Pa]
Outlet pressure	$2 \times 10^5$ [Pa]
Inlet temperature	873.15 [K]
Outlet temperature	1111.15 [K]

Cokes density

1600 [kg/m<sup>3</sup>]

Thermal conductivity of the coke

0.00645 [kJ /(m s K)]

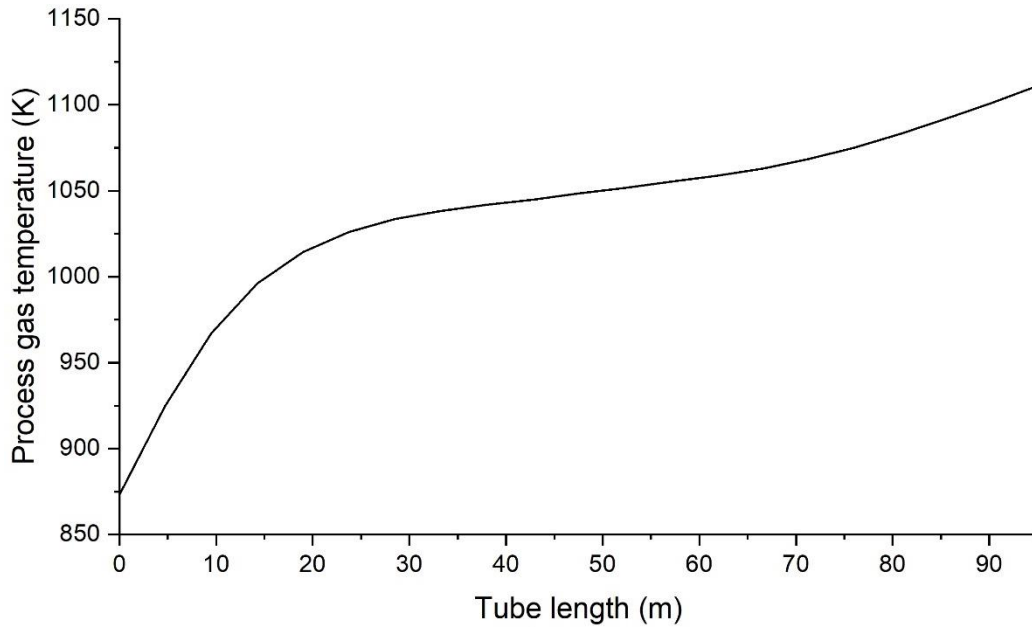


**Fig. 4.** Process gas temperature profile [15]

### 3.2 Validation under clean tube condition

Firstly, the industry data of propane conversion and main products yields reported by Van Damme et al. [36] under clean tube condition were used to validate the 1-D pseudo-dynamic PFR model. As can be seen in Table 3, the simulation results under clean tube condition are in good agreement with industrial data.

**Table 3.** Simulation results of propane conversion and main products yields compared with industrial data (clean tube condition)

Product	Simulation results	Industrial data	Relative error
Propane conversion	87.91%	90.06%	-2.38%
C <sub>2</sub> H <sub>4</sub>	35.80%	34.50%	3.16%
C <sub>3</sub> H <sub>6</sub>	14.77%	14.70%	0.50%
CH <sub>4</sub>	25.31%	24.00%	5.46%

### 1 3.3 Validation with 700 hours run length

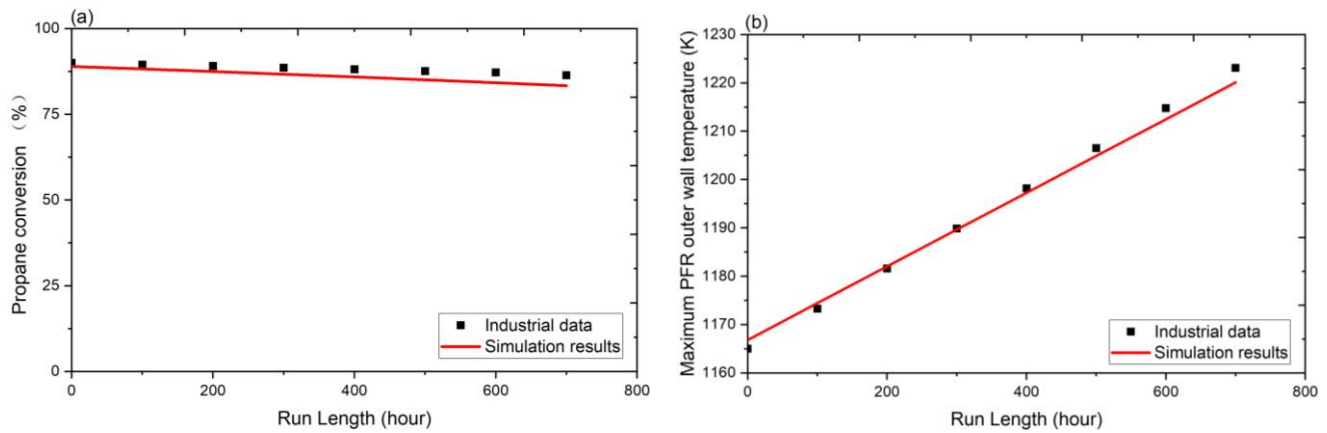
2 The coke formation on the PFR inner tube wall with time will affect the PFR performance by reducing  
3 diameter and increasing total thermal resistance [8]. As a result, the propane conversion decreases with  
4 time because less time for reaction and higher outer wall temperature profile will be needed to keep the  
5 same process gas temperature profile.

6 In this study, the PFR model has been run for 700 hours. The highest coke thickness occurred at the  
7 PFR outlet because of the highest temperature. As a result, the coke at the PFR outlet affects the PFR  
8 performance most significantly [5]. To validate the performance of PFR with time, coke thickness at the  
9 PFR outlet after running the reactor for 100 hours, 300 hours and 700 hours were compared with the  
10 industrial data and shown in Table 4. As can be seen from Table 4, the pseudo-dynamic model can  
11 predict the coke formation accurately compared with the industrial data.

12 **Table 4.** Simulation results of PFR outlet coke thickness compared with industrial data

Run length	Simulation results	Industrial data	Relative error
100 hours	0.13 cm	0.14 cm	-7.1%
300 hours	0.41 cm	0.44 cm	-6.8%
700 hours	0.94 cm	0.98 cm	-4.08%

13 It can be seen from Fig. 5(a) that the propane conversion change with time predicted by the pseudo-  
14 dynamic model shows good agreement with the data from industry. The needed outer wall temperature  
15 of PFR increases with time since the coke formation increases the total thermal resistance [8]. Similar as  
16 the coke thickness, maximum outer wall temperature is needed at the PFR outlet. The simulated  
17 maximum outer wall temperature change with time shows good agreement with the industrial data as  
18 presented in Fig. 5(b). These results show that the pseudo-dynamic model can predict the PFR  
19 performance accurately. Therefore, it can be used for further process analysis.



1

2 **Fig. 5.** Simulation results compared with industrial data: (a) propane conversion (b) maximum outer wall  
 3 temperature (at PFR outlet)

#### 4 4. Methodology for cost-benefit analysis and exergy analysis

5 This section aims to look at the impact of diluent-to-propane ratio of different diluents on the process  
 6 performance. In this study, the total inlet mass flow rate of process gas (propane + diluent) is fixed at  
 7 1.0689 kg/s and inlet pressure is fixed at 3 bars, which are the same as the base case used to validate  
 8 the model. The diluent-to-propane ratio varies from 0.2-1.0, which is the operating range reported by  
 9 Sundaram and Froment [17]. Process gas temperature profile was kept constant and the same as shown  
 10 in Fig. 4, which means the required outer wall temperature will increase with time because of the coke  
 11 formation.

##### 12 4.1 Cost-benefit analysis

13 To evaluate the impact of diluent-to-propane ratio, propane conversion and valuable products yields  
 14 under clean tube condition, coking rate, run length of the PFR, annual production of valuable products,  
 15 annual energy consumption and annual profit of the PFR at different diluent-to-propane ratios are  
 16 simulated and discussed. For the run length, the PFR assumed to be shut down for decoking when the  
 17 coke thickness reaches 0.0135 m as reported by Sundaram and Froment [15].

18 The annual production of valuable products can reflect the yearly production capacity of PFR considering  
 19 the outlet flowrates of valuable products change with time and run length. The yearly production time is

1 assumed 8160 hours as reported in several literatures[5, 8]. Annual production of valuable products can  
 2 be calculated by the following equation:

$$3 \quad F_{i \text{ annual}} = 8160 \times \frac{F_{i \text{ total}}}{t_c + t_d} \quad (13)$$

4 Annual energy consumption can be used to reflect the energy cost of PFR in quantity and calculate the  
 5 annual profit. It can be determined by the following equation:

$$6 \quad \dot{Q}_{\text{annual}} = 8160 \times \frac{\dot{Q}_{\text{total}}}{t_c + t_d} \quad (14)$$

7 The annual profit of the PFR will consider the parameters listed in Table 5 and calculated by the following  
 8 equations:

$$9 \quad P_{\text{annual}} = INC_{\text{annual}} - COS_{\text{annual}} \quad (15)$$

$$10 \quad INC_{\text{annual}} = \sum F_{i \text{ annual}} \times COS_i \quad (16)$$

$$11 \quad COS_{\text{annual}} = \frac{t_c}{t_c + t_d} \left( F_{\text{Propane}}(z = 0) \times COS_{\text{Propane}} + F_d(z = 0) \times COS_{\text{diluent}} + \dot{Q}_{\text{annual}} \times COS_{\text{Heat}} + \frac{DCC}{t_c} \right) * 8160 \quad (17)$$

12 **Table 5.** Parameters for calculating annual profit [6]

Parameters	Physical meaning	Values	Units
$t_d$	Decoking time per cycle	48	[hr]
$COS_{\text{Propane}}$	Propane price factor	0.596	[\$/kg]
$COS_{\text{Ethylene}}$	Ethylene price factor	1.356	[\$/kg]
$COS_{\text{Propylene}}$	Propylene price factor	1.576	[\$/kg]
$COS_{\text{Steam}}$	Steam price factor	0.0129	[\$/kg]
$COS_{\text{carbon dioxide}}$	Carbon dioxide price factor	0	[\$/kg]
$COS_{\text{heat}}$	Heat price factor	$1.26 \times 10^1$	[\$/GJ]

Parameters	Physical meaning	Values	Units
<i>DCC</i>	Decoking cost per cycle	66,000	[\$]

1

## 2 4.2 Exergy analysis

3 Exergy analysis can be used to identify the energy cost of PFR in quality [19]. Similar as material and  
4 energy balances, there is no accumulation of exergy in the PFR due to the low residence time. The exergy  
5 balance of PFR is shown in Eq. (18).

$$6 \quad \dot{E}_Q + \dot{E}_{f,in} = \dot{E}_{f,out} + \dot{E}_D \quad (18)$$

7  $\dot{E}_Q$  is the exergy of required heat which can be determined by the Eq. (19),  $\dot{E}_{f,in}$  and  $\dot{E}_{f,out}$  are the exergy  
8 of inlet and outlet process gas, and  $\dot{E}_D$  is the exergy destruction.

$$9 \quad \dot{E}_Q = \sum_{z=0}^L \frac{Q(z)}{L} \times \left( 1 - \frac{T_{we}(z)}{T} \right) \quad (19)$$

10 For the stream of PFR, only physical exergy ( $\dot{E}^{ph}$ ) and chemical exergy  $\dot{E}^{ch}$  are considered [4]. The  
11 exergy of stream of PFR can be determined by the following equations:

$$12 \quad \dot{E}_f = \dot{E}^{ph} + \dot{E}^{ch} \quad (20)$$

13 The physical exergy of the process gas along the PFR can be determined by the following equation:

$$14 \quad \dot{E}^{ph}(z) = H(T(z), P(z), x(z)) - H(T_0, P_0, x(z)) - T_0 \left( S(T(z), P(z), x(z)) - S(T_0, P_0, x(z)) \right) \quad (21)$$

15 Where,  $H(z)$  and  $S(z)$  are the enthalpy and entropy of process gas at the position  $z$  along the PFR.  $T_0$  and  
16  $P_0$  are the temperature and pressure of reference environmental state, which is assumed to be the natural  
17 environment (298.15K, 1.01\*10<sup>5</sup>Pa) of thermal cracking furnace in this work.

18 The chemical exergy of the process gas along the PFR can be determined by the following equation:

$$19 \quad \dot{E}^{ch}(z) = \sum_{i=1}^{NC} x_i(z) \times (\dot{E}_i^0 + RT_0 \ln x_i(z)) \times \sum_{i=1}^{NC} \frac{F_i(z)}{MW_i} \quad (22)$$

1 Where  $x_i$  is the mole fraction of component i and  $\dot{E}_i^0$  is the molar standard chemical exergy of component  
 2 i which can be determined by:

$$3 \quad x_i(z) = \frac{F_i(z)/MW_i}{\sum_{i=1}^{NC} F_i(z)/MW_i} \quad (23)$$

$$4 \quad \dot{E}_i^0 = \Delta G_f^0 + \sum_{k=1}^{NE} n_{i,k} \dot{E}_k^0 \quad (24)$$

5 Where  $\Delta G_f^0$  is the standard Gibbs energy of formation and  $\dot{E}_k^0$  is the standard chemical exergy value of  
 6 elements k. Chemical exergy of reference substances was firstly determined by Szargut et al. [37] and  
 7 then developed by Rivero and Garfias [38].

8 The exergy of inlet stream (z=0) and outlet stream (z=L) can be determined with the calculated physical  
 9 exergy and chemical exergy along the PFR. Then the exergy destruction of the PFR can be determined.

10 The exergy destruction of PFR can be divided into the exergy destruction caused by heat transfer ( $\dot{E}_{D,ht}$ )  
 11 and the exergy destruction caused by the thermal cracking reactions ( $\dot{E}_{D,re}$ ). These two kinds of exergy  
 12 destruction can be calculated by the following equations:

$$13 \quad \dot{E}_{D,ht} = \dot{E}_Q - \sum_{z=0}^L \frac{Q(z)}{L} \times \left(1 - \frac{T(z)}{T}\right) \quad (25)$$

$$14 \quad \dot{E}_{D,re} = \dot{E}_D - \dot{E}_{D,ht} \quad (26)$$

15 Since the exergy of required heat is much smaller than the exergy of stream, the conventional exergy  
 16 efficiency is almost equal to 100%, the rational exergy efficiency is used in this study to analyse the  
 17 exergy efficiency of PFR [39]. The rational exergy efficiency can be calculated by Eq. (27).

$$18 \quad \varepsilon = \frac{\dot{E}_{f,out} - \dot{E}_{f,in}}{\dot{E}_Q} \quad (27)$$

19 To evaluate the exergy performance of PFR combined with coke formation, annual exergy of required  
 20 heat ( $\dot{E}_{Q,annual}$ ), annual exergy destruction ( $\dot{E}_{D,annual}$ ) and annual average exergy efficiency ( $\varepsilon_{annual}$ )  
 21 can be determined by the following equations:

$$\dot{E}_{Q,annual} = 8160 \times \frac{\dot{E}_{Q,total}}{t_c + t_d} \quad (28)$$

$$\dot{E}_{D,annual} = 8160 \times \frac{\dot{E}_{D,total}}{t_c + t_d} \quad (29)$$

$$\varepsilon_{annual} = 1 - \frac{\dot{E}_{D,annual}}{\dot{E}_{Q,annual}} \quad (30)$$

## 5. Results and discussions on impact of diluent-to-propane ratio

### 5.1 Impact of diluent-to-propane ratio using steam as diluent

Steam is the most commonly used diluent in ethylene manufacturing. Therefore, the impact of diluent-to-propane ratio using steam as diluent has been first analysed.

The propane conversion with different steam-to-propane ratios under clean tube condition is shown in Fig. 6. The propane conversion decreases from 89.2% to 85.5% when the steam-to-propane ratio increases from 0.2 to 1.0. Propane conversion is mainly determined by primary reaction rate. Higher steam-to-propane ratio can reduce the hydrocarbon partial pressure, which leads to the decrease of primary reaction rate according to the Arrhenius law.

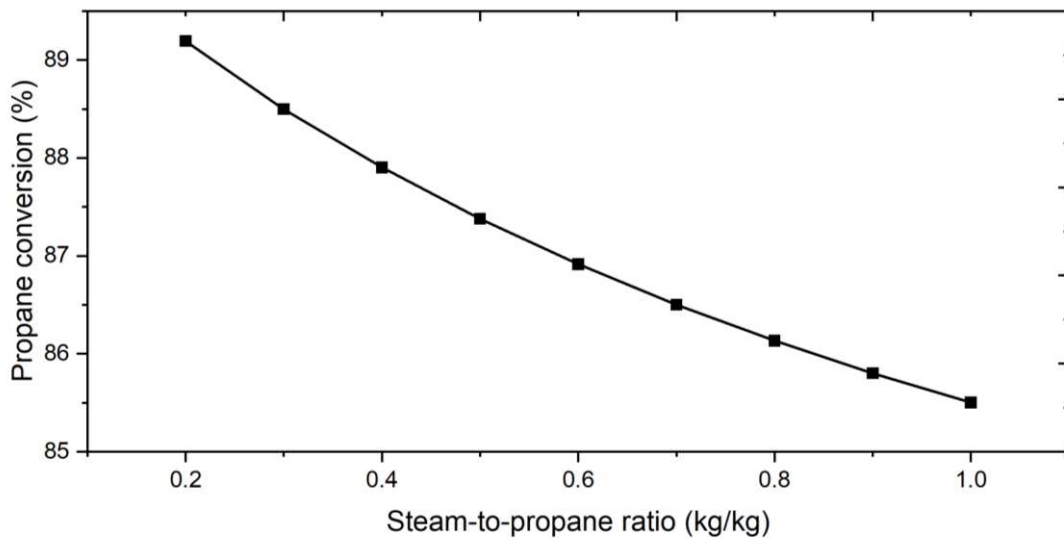
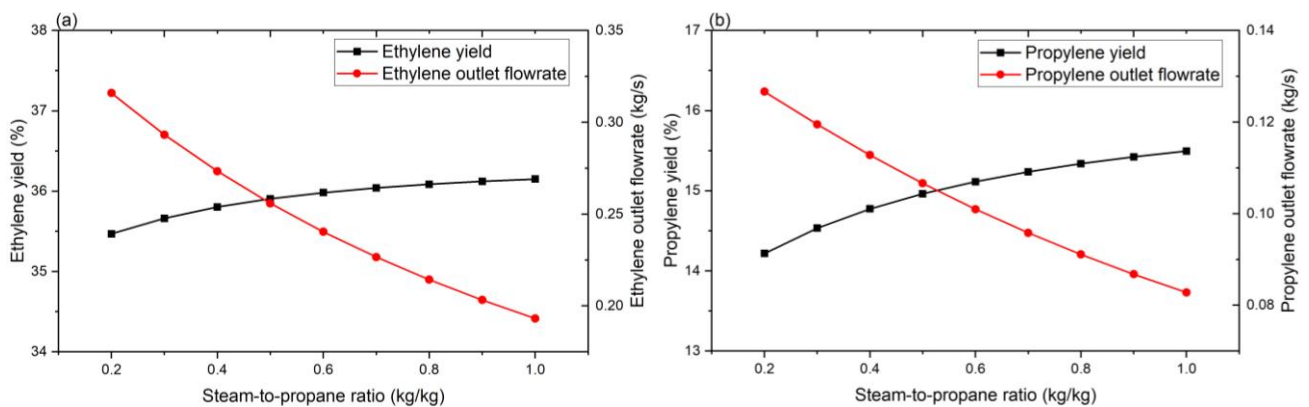
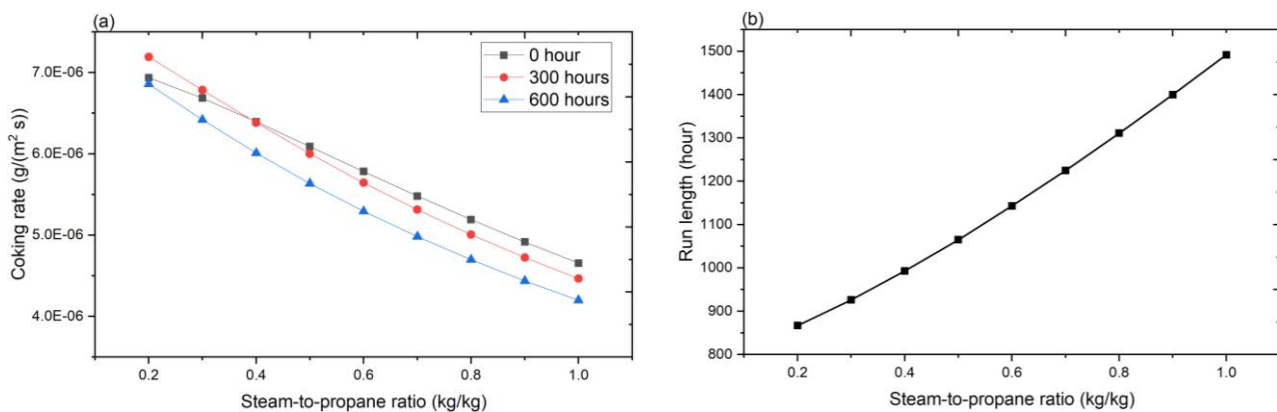


**Fig. 6.** Propane conversion under clean tube conditions using steam as diluent

1 As presented in Fig. 7, the increase of steam-to-propane ratio leads to a slightly increase of valuable  
 2 products yields including ethylene from 35.47% to 36.15% and propylene from 14.22% to 15.50% under  
 3 clean tube condition. The impact can be explained by the fact that increase of hydrocarbons partial  
 4 pressure can reduce the reaction rates of undesired secondary reactions. However, with the increase of  
 5 steam-to-propane ratio, the inlet mass flow rate of the propane decreases since the total inlet mass flow  
 6 rate is fixed at 1.0689 kg/s. As a result, the outlet flow rates of both ethylene and propylene under clean  
 7 tube condition decrease significantly as shown in Fig. 7.



8  
 9 **Fig. 7.** Valuable products yields and outlet flowrate under clean tube conditions using steam as diluent:  
 10 (a) ethylene (b) propylene

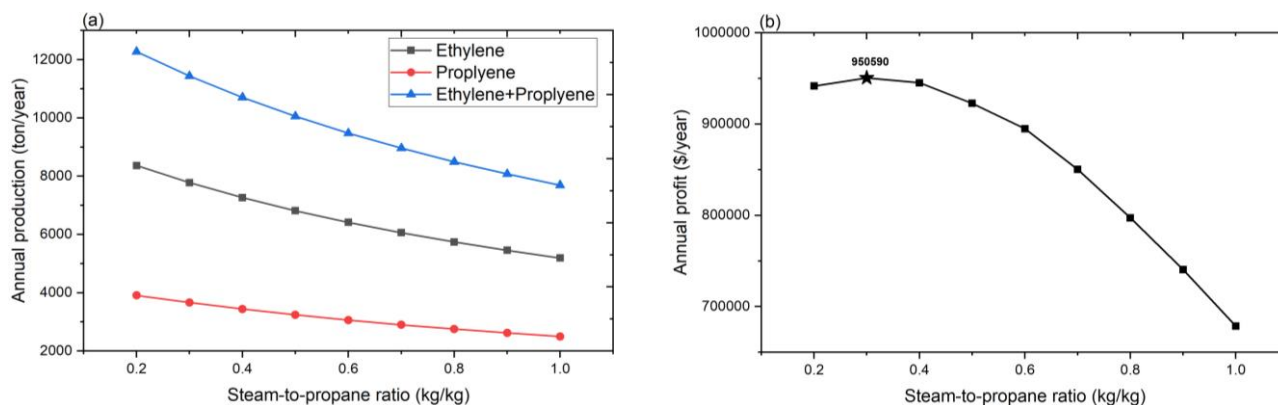


11  
 12 **Fig. 8.** (a) Coking rate at PFR outlet at different operating hours and (b) run length of PFR using steam  
 13 as diluent

14 To evaluate the dynamic impact of steam-to-propane ratio, the coking rate at the PFR outlet under clean  
 15 tube condition, at 300 hours and 600 hours are presented in Fig. 8(a). The coking rate at PFR outlet is

1 the most important since the outlet always has the thickest coke layer, which directly determines the run  
 2 length of PFR. The concentration of propylene, which is considered as coke precursor in this model,  
 3 decreases with the increase of steam-to-propane ratio. Therefore, it can be found from Fig. 8(a) that the  
 4 coking rate at PFR outlet at different time always decreases with the increase of steam-to-propane ratio.  
 5 The coking rate at the same steam-to-propane ratio also changes with time because of the increase of  
 6 propylene concentration and the reduction of PFR volume. When the steam-to-propane ratio varying from  
 7 0.2 to 0.3, the propylene concentration is very low because of the high reaction rate of secondary  
 8 reactions. As a result, the coking rate increases in the first 300 hours since the impact of the increase of  
 9 propylene concentration is more significant. As the coking rate decreases, the run length of PFR  
 10 increases significantly from 867 hours to 1492 hours when the ratio increases from 0.2-1.0 as shown in  
 11 Fig.8(b).

12 As the PFR operating with higher steam-to-propane ratio has longer run length but lower valuable  
 13 products outlet flowrate, annual production is used to analyse the yearly production capacity of PFR  
 14 considering these two different kinds of impact. The annual production is calculated from Eq. (13)  
 15 considering the outlet flowrate change with time and shut-down time for decoking.



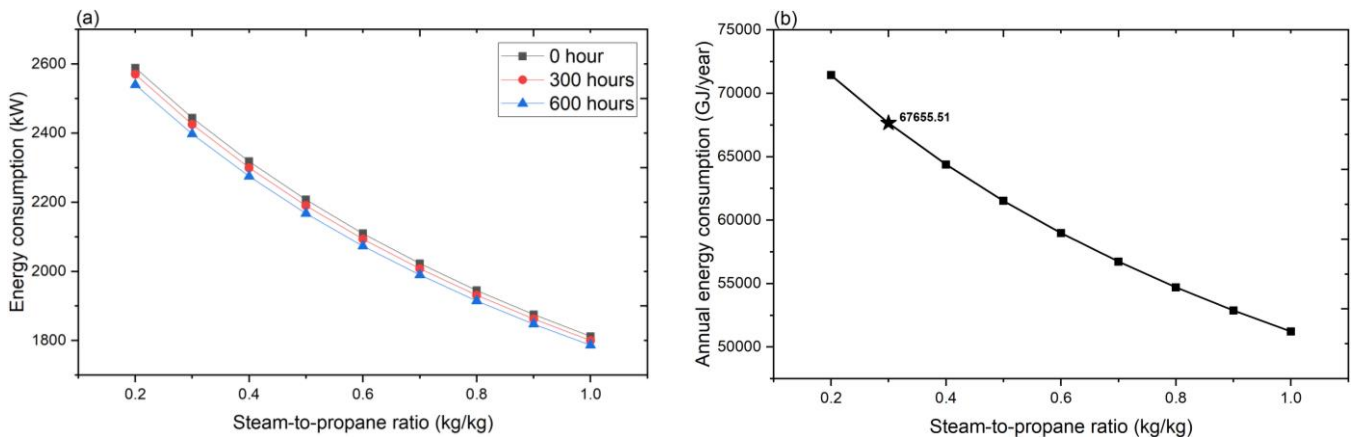
17 **Fig. 9.** (a) Annual production and (b) annual profit of PFR using steam as diluent

18 As shown in Fig. 9(a), although the run length is longer, both ethylene and propylene annual productions  
 19 are lower when the PFR operating with higher steam-to-propane ratio. The annual production of total  
 20 valuable products (ethylene + propylene) decreases from 12,273 ton/year to 7,689 ton/year when the  
 21 steam-to-propane ratio increases from 0.2 to 1.0. It is obvious that low steam-to-propane ratio is preferred

1 when only considering the annual production of valuable products. However, loss in valuable product  
 2 yields, higher decoking cost because of short run length and higher energy consumption for higher  
 3 propane inlet mass flowrate cannot be neglected when considering the economic benefits of PFR  
 4 operation. To consider all the above impact, annual profit of PFR with different steam-to-propane ratios  
 5 are calculated according to Eq. (15)-(17) and parameters listed in Table 5.

6 As shown in Fig. 9(b), the PFR can get a high annual profit when steam-to-propane ratio varying from  
 7 0.2 to 0.4. The highest annual profit is 950,590 \$/year when the operating steam-to-propane ratio of PFR  
 8 is 0.3. At this ratio, the PFR has longer run length, higher valuable products yields and lower energy  
 9 consumption compared with lower steam-to-propane ratio. The annual profit of PFR decreases  
 10 significantly from 922,680 \$/year to 678,665 \$/year when the steam-to-propane ratio increases from 0.5  
 11 to 1.0. In this range, the decrease in annual production of valuable products plays a decisive role in  
 12 annual profit.

13 As shown in Fig.10(a), the energy consumption of PFR decreases at different operating hours when the  
 14 steam-to-propane ratio increases from 0.2 to 1.0. The energy consumption decreases with the increase  
 15 of steam-to-propane ratio due to (1) less energy is used to heat the process gas because the specific  
 16 heat capacity of propane is higher than that of steam (2) less mass flowrate of propane taking part in  
 17 thermal cracking reactions. The energy consumption also decreases with operating hours at different  
 18 steam-to-propane ratios. It can be explained by the coke formation with time, which reduce the energy  
 19 consumption of thermal cracking reactions by reducing the PFR volume.



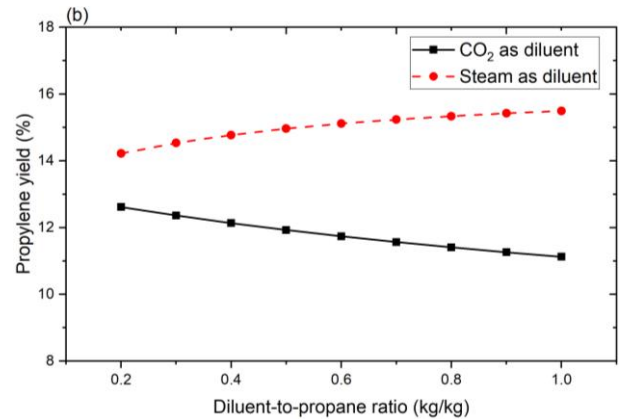
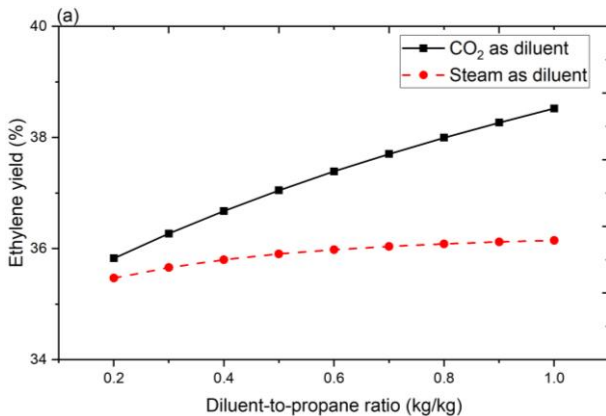
1 **Fig.10.** (a) Energy consumption at different operating hours and (b) annual energy consumption of PFR  
2 using steam as diluent

3 Similar as the annual production and annual profit, the annual energy consumption can be used to  
4 analyse the thermodynamic performance of the PFR considering both the energy consumption change  
5 with time and different run lengths at different steam-to-propane ratios. As presented in Fig.10(b), the  
6 annual energy consumption of PFR decreases with the increase of steam-to-propane ratio. The annual  
7 energy consumption when operating at the steam-to-propane ratio 0.3, which can achieve the highest  
8 annual profit, is 67655.51GJ. Although the annual energy consumption is significantly lower when  
9 operating at higher steam-to-propane ratio, the loss in annual production and profit is unacceptable.

## 10 5.2 Impact of diluent-to-propane ratio using CO<sub>2</sub> and compared with using steam

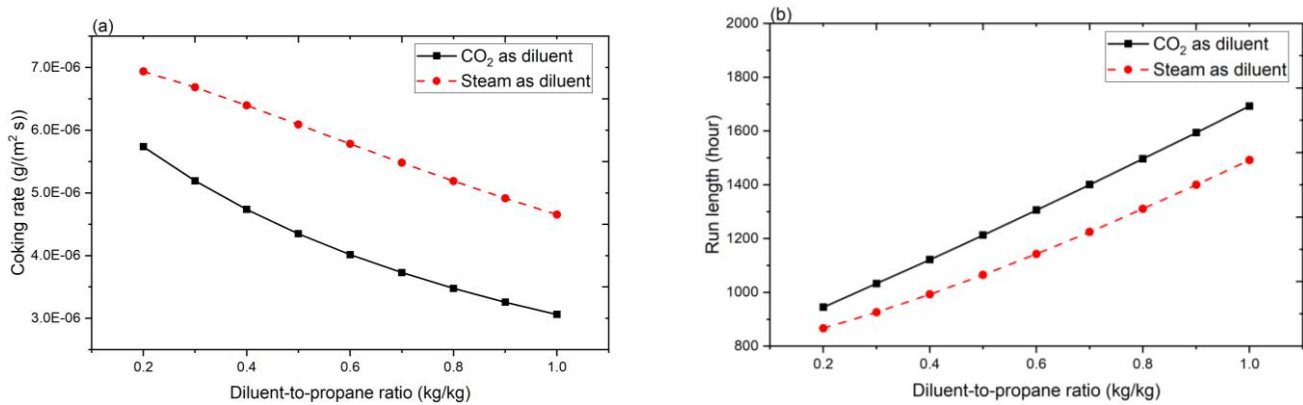
### 11 5.2.1 Cost-benefit analysis

12 The yields of valuable products with different diluent-to-propane ratios under clean tube condition using  
13 CO<sub>2</sub> and steam are analysed and presented in Fig. 11. Higher yield means higher outlet flowrate when  
14 comparing the two kinds of diluents at the same ratio since the mass flowrate of propane is the same.  
15 Compared with steam, CO<sub>2</sub> has a higher molecular weight. Therefore, at the same diluent-to-propane  
16 ratio, the molar flowrate of CO<sub>2</sub> is smaller. It leads to a higher partial pressure of propylene and more  
17 propylene participates in the reaction to produce ethylene and methane. As a result, using CO<sub>2</sub> as diluent  
18 can get a higher ethylene yield and lower propylene yield for different diluent-to-propane ratios, which  
19 can be found from Fig. 11.



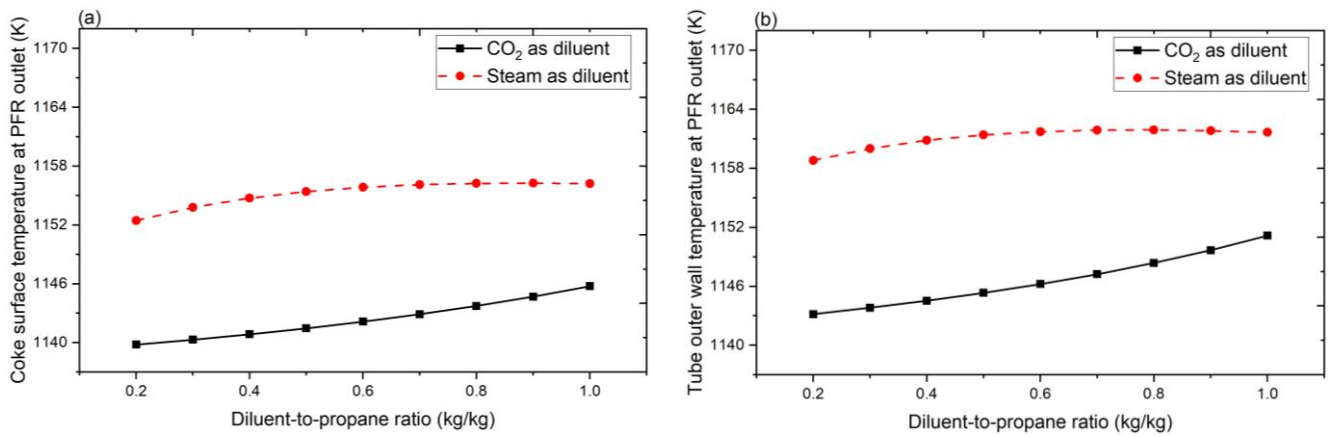
1 **Fig. 11.** Comparison of valuable products yields under clean tube condition using CO<sub>2</sub> and steam: (a)  
 2 ethylene (b) propylene

3 From Fig. 8(a), it can be observed that the coking rate at 3 different time (e.g. 0 hour, 300 hours and 600  
 4 hours) has similar trend when diluent-to-propane ratio varying from 0.2-1.0. Therefore, only the coking  
 5 rates at PFR outlet under clean tube condition using CO<sub>2</sub> and steam are compared here.



6  
 7 **Fig. 12.** Comparison of (a) coking rate under clean tube condition and (b) run length of PFR using CO<sub>2</sub>  
 8 and steam

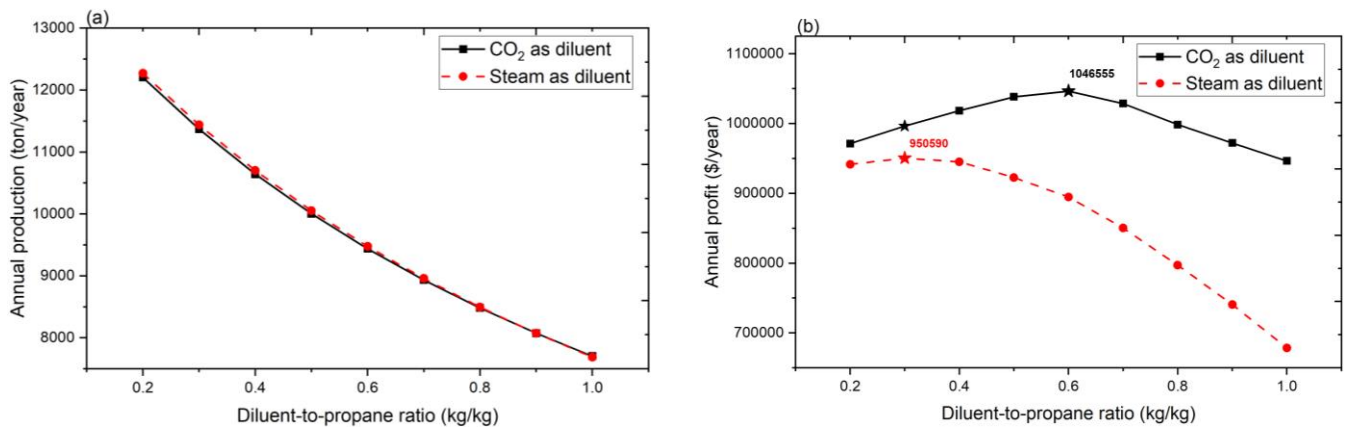
9 Fig. 12 indicates that using CO<sub>2</sub> can reduce the coking rate at different diluent-to-propane ratios  
 10 compared with using steam. The coking rate is controlled by propylene concentration and coke surface  
 11 temperature according to Eq. (3). Although using CO<sub>2</sub> increases the partial pressure of propylene, the  
 12 coke surface temperature at PFR outlet is significantly lower when using CO<sub>2</sub>. It can be explained by the  
 13 lower specific heat capacity of CO<sub>2</sub>. As the temperature profile of process gas is fixed in this study, lower  
 14 tube outer wall temperature is required to heat the process gas when using CO<sub>2</sub> as diluent. As a result,  
 15 the coke surface temperature is also lower when the heat is transferred from tube outer wall to coke  
 16 surface. The coke surface temperature and tube outer wall temperature at PFR outlet under clean tube  
 17 condition are shown in Fig. 13. Since using CO<sub>2</sub> as diluent can reduce coking rate, it can increase the  
 18 run length of PFR significantly. Fig. 12(b) indicates that the run length of PFR can be increased  
 19 prominently by 79 hours (9.1%) at diluent-to-propane ratio 0.2 and 202 hours (13.5%) at diluent-to-  
 20 propane ratio 1.0. Replacing steam with CO<sub>2</sub> as diluent increase the run length of PFR more significantly  
 21 at higher diluent-to-propane ratios.



1

2 **Fig. 13.** Comparison of temperature of different layers (at PFR outlet) under clean tube condition using  
 3 CO<sub>2</sub> and steam: (a) coke surface (b) tube outer wall

4 The total annual production of valuable products using CO<sub>2</sub> and steam will be compared to  
 5 comprehensively evaluate the yearly production capacity of PFR. As presented in Fig. 14(a), the annual  
 6 production using CO<sub>2</sub> as diluent is almost the same as that using steam as diluent. The highest annual  
 7 production at diluent-to-propane ratio 0.2 only decreases by 0.56% from 12,272 ton/year to 12,203  
 8 ton/year when replacing steam with CO<sub>2</sub> as diluent. Although using CO<sub>2</sub> as diluent will reduce the yield  
 9 of propylene compared with using steam, the increase of ethylene yield and run length are beneficial for  
 10 increasing annual production of valuable products.



11

12 **Fig. 14.** Comparison of (a) annual production and (b) annual profit of PFR using CO<sub>2</sub> and steam

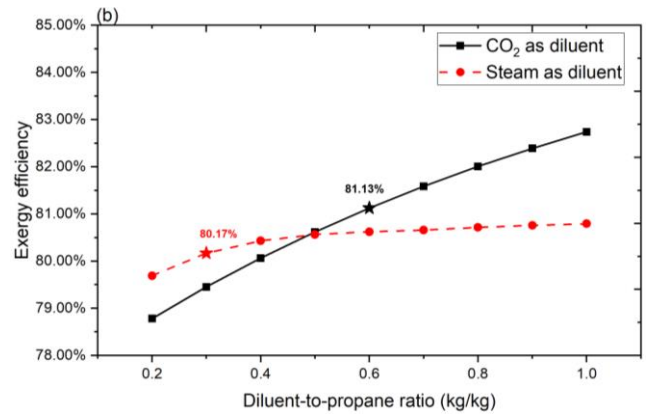
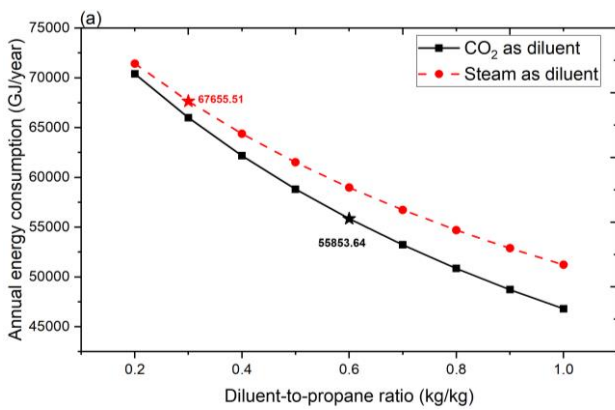
13 With similar annual production, longer run length (shown in Fig. 12), lower annual energy consumption  
 14 (shown in Fig. 15(a)) and lower cost of diluent (shown in Table 5) can be obtained by using CO<sub>2</sub> compared

1 with steam as diluent. As a result, replacing steam with CO<sub>2</sub> as diluent can significantly increase the  
 2 annual profit of PFR. Fig. 14(b) indicates that the highest annual profit can be reached when the PFR  
 3 operating at diluent-to-propane ratio 0.6 when using CO<sub>2</sub> as diluent. This highest annual profit is 10.10%  
 4 higher than the highest annual profit using steam as diluent at diluent-to-propane ratio 0.3.

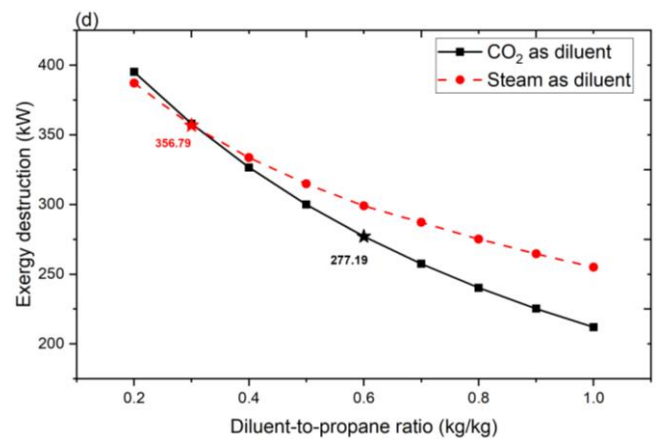
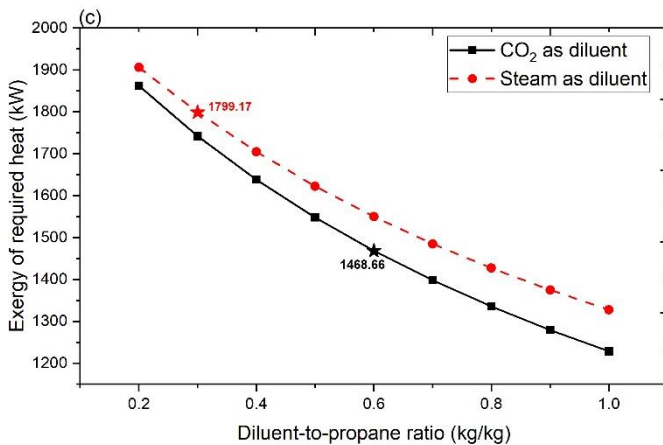
5 **5.2.2 Energy and exergy analysis**

6 The annual energy consumption using CO<sub>2</sub> and steam are analysed and presented in Fig.15(a). Although  
 7 using CO<sub>2</sub> can increase the run length of PFR, it can still reduce the annual energy consumption because  
 8 using CO<sub>2</sub> as diluent can reduce the heat required to maintain the temperature profile of the process gas.  
 9 By comparing the operating diluent-to-propane ratio to achieve the highest annual profit, using CO<sub>2</sub> can  
 10 reduce the annual energy consumption by 11801.87GJ (17.44%).

11

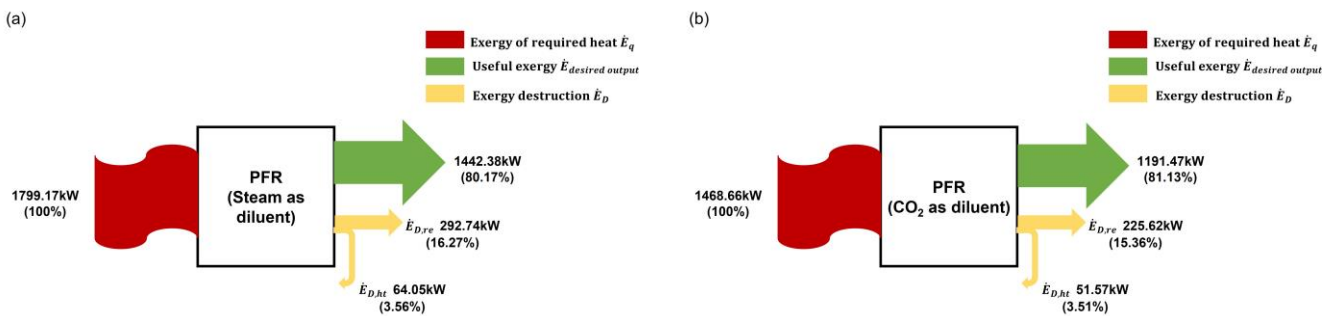


12



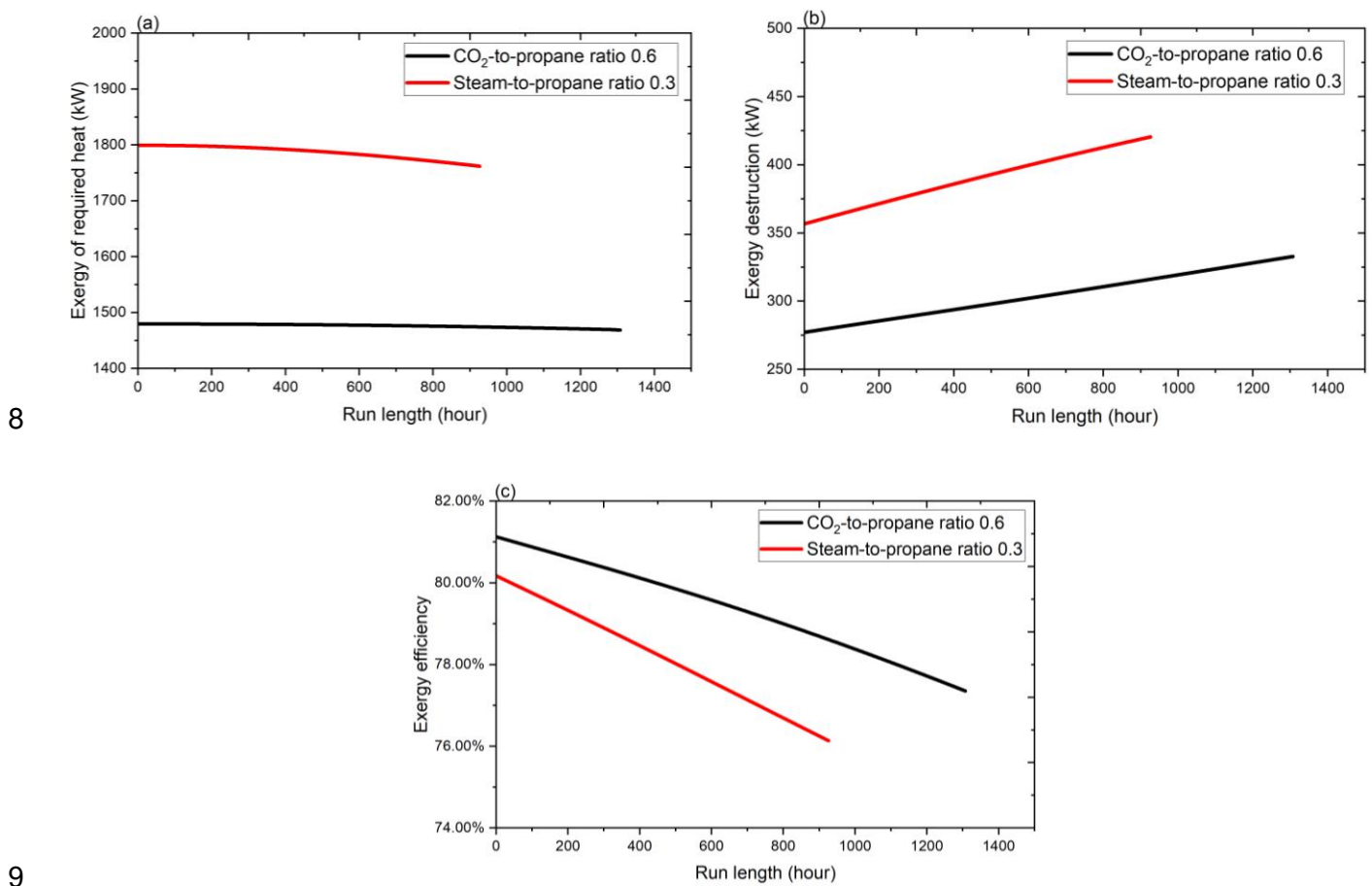
13 **Fig.15.** Comparison of (a) annual energy consumption (b) exergy efficiency under clean tube condition  
 14 (c) exergy of required heat under clean tube condition (d) total exergy destruction under clean tube  
 15 condition using CO<sub>2</sub> and steam

1 The exergy destruction inside PFR is caused by the temperature difference between tube outer wall and  
 2 process gas and the thermal cracking reactions, the exergy efficiency of PFR using CO<sub>2</sub> and steam as  
 3 diluent under clean tube condition are analysed and presented in Fig.15(b). For both steam and CO<sub>2</sub> as  
 4 diluent, exergy efficiencies of the PFR slightly increase with the increase of diluent-to-propane ratios.  
 5 Higher diluent-to-propane ratio means less mass flowrate of propane in the process gas, so the exergy  
 6 destruction caused by the thermal cracking reactions decreases. When the diluent-to-propane ratio  
 7 varying from 0.2 to 0.4, the exergy efficiency of using CO<sub>2</sub> as diluent is lower than that using steam as  
 8 diluent. When the PFR operating in this range of diluent-to-propane ratio, the reaction rate of both primary  
 9 reactions and secondary reactions is much higher when using CO<sub>2</sub> because of higher hydrocarbon partial  
 10 pressure. When the diluent-to-propane ratio increasing from 0.5 to 1.0, the exergy destruction of reactions  
 11 decreases rapidly and the lower temperature difference between tube outer wall and process gas using  
 12 CO<sub>2</sub> as diluent make the exergy efficiency higher. Although the change in exergy efficiency is tiny, using  
 13 CO<sub>2</sub> as diluent can reduce the exergy of required heat and total exergy destruction of the PFR which are  
 14 presented in Fig.15 (c) and Fig.15 (d). It can be explained by the less heat required and lower tube outer  
 15 wall temperature when using CO<sub>2</sub> as diluent. When the PFR operating with the ratio can achieve highest  
 16 annual profit, using CO<sub>2</sub> as diluent can increase the exergy efficiency of PFR under clean tube condition  
 17 by 0.96%, reduce the exergy of required heat by 330.51kW (18.37%) and reduce the total exergy  
 18 destruction by 79.60kW (22.31%).



19  
 20 **Fig.16.**Exergy utilization in the PFR using (a) steam and (b) CO<sub>2</sub> as diluent operating at the ratio  
 21 achieving highest annual profit under clean tube condition

1 The exergy utilization of two different kinds of diluents operating at the ratio achieving highest annual  
 2 profit under clean tube condition are shown in Fig.16. The exergy destruction of PFR is divided into the  
 3 exergy destruction caused by heat transfer ( $\dot{E}_{D,ht}$ ) and the exergy destruction caused by the thermal  
 4 cracking reactions ( $\dot{E}_{D,re}$ ). By comparing of these two cases, using CO<sub>2</sub> operating at the diluent-to-  
 5 propane ratio 0.6 can reduce the (1)  $\dot{E}_{D,re}$  because of less exergy of required heat and lower mass flow  
 6 rate of propane in process gas (2)  $\dot{E}_{D,ht}$  because of less exergy of required heat and lower temperature  
 7 difference between tube outer wall and process gas.



10 **Fig.17.** Comparison of (a) exergy of required heat (b) exergy destruction (c) exergy efficiency with time  
 11 when PFR operating at the diluent-to-propane ratio with highest annual profit using CO<sub>2</sub> and steam  
 12 When operating at the diluent-to-propane ratio for highest annual profit and considering the coke  
 13 formation, using CO<sub>2</sub> as diluent required lower exergy in heat, make lower exergy destruction and has a  
 14 higher exergy efficiency. during the whole run length presented in Fig.17 The exergy of required heat

1 decreases with time since the required heat decreases with time (shown in Fig.10 (a)).As presented in  
 2 Fig.17(b), the exergy destruction increases with time despite the decrease of exergy of required heat  
 3 because the coke formation increases the thermal resistance from tube outer wall to process gas. As a  
 4 result, the exergy efficiency decreases with time shown in Fig.17(c).

5 The annual exergy of required heat, annual exergy destruction and annual average exergy efficiency are  
 6 shown in Table.6.

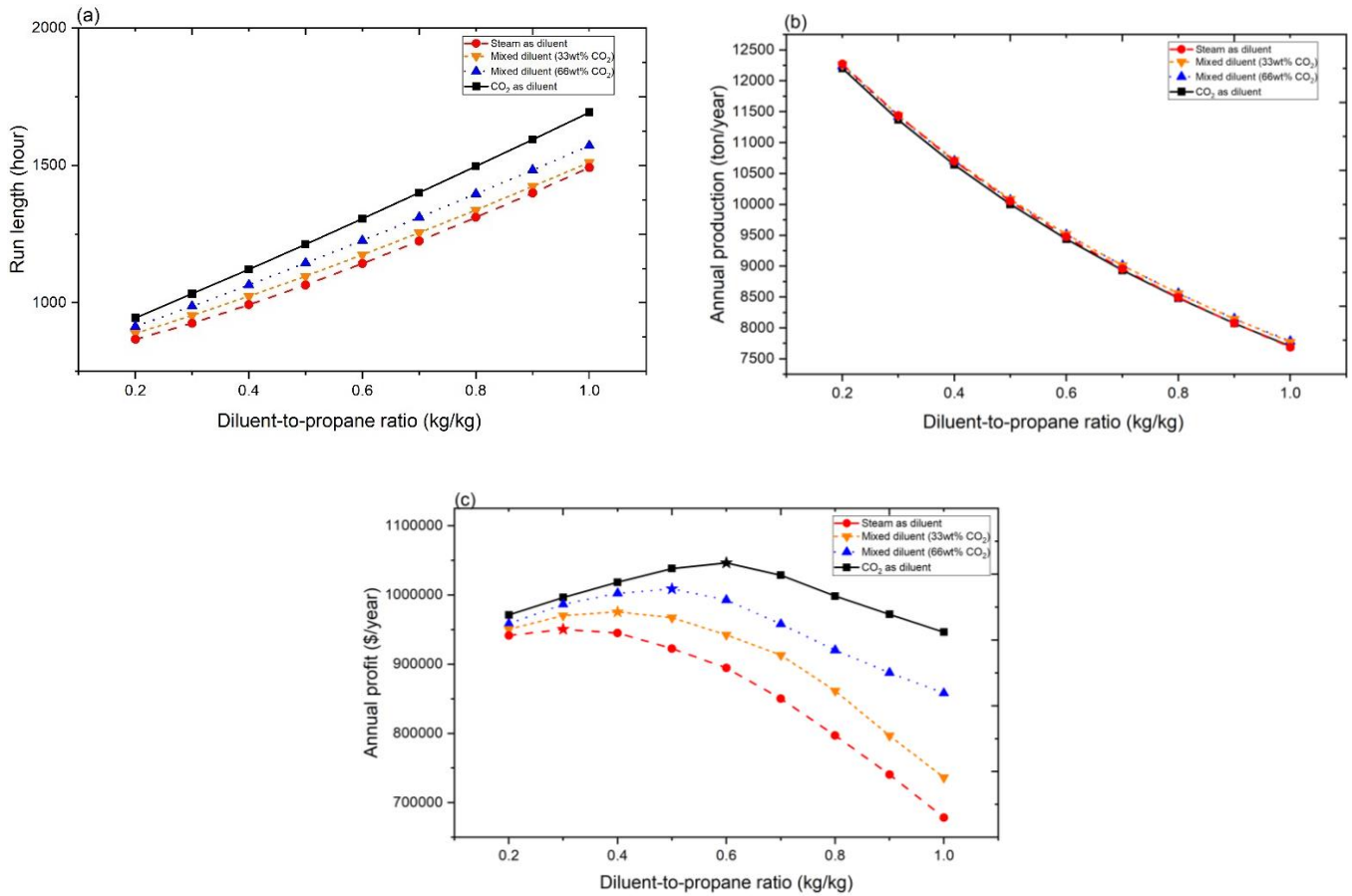
7 **Table 6.** Comparison of annual exergy utilization when PFR operating at the diluent-to-propane ratio  
 8 with highest annual profit using CO<sub>2</sub> and steam

	Run length (hour)	Annual exergy of required heat (GJ)	Annual exergy destruction (GJ)	Annual average exergy efficiency (%)
Steam as diluent	926	49896	10872	78.18
CO <sub>2</sub> as diluent	1307	41832	8640	79.36
Absolute difference	381	-8064	-2232	1.18
Relative difference	29.15%	-16.16%	-20.53%	1.50%

9

### 10 5.3 Comparison of pure/mixed diluent in 4 different scenarios

11 Four scenarios of pure/mixed diluent using steam and CO<sub>2</sub> have been analysed. The following scenarios:  
 12 (a) Steam only; (b) Mixed diluent (67wt% steam ,33wt% CO<sub>2</sub>); (c) Mixed diluent (33wt% steam, 67wt %  
 13 CO<sub>2</sub>); (d) CO<sub>2</sub> only are designed to compare the key performance indicators of pure diluent, mixed diluent  
 14 with more steam and mixed diluent with more CO<sub>2</sub>.



1

2

3 **Fig. 18.** Comparison of key performance indicators of PFR of 4 different scenarios: (a) run length (b)  
 4 annual production (c) annual profit

5 As presented in Fig. 18, higher mass fraction of CO<sub>2</sub> in diluent can help the PFR to increase the run  
 6 length at different diluent-to-propane ratios. It can be explained by the lower coke surface temperature  
 7 when using CO<sub>2</sub> as discussed before. The annual productions of 4 different scenarios all reach the  
 8 highest value at diluent-to-propane ratio 0.2 and they are quite close. These 4 highest values are  
 9 compared and shown in Fig. 18. The highest annual profits for the 4 different scenarios are reached at  
 10 different ratios. The higher mass fraction of CO<sub>2</sub> in diluent required a higher diluent-to-propane ratio to  
 11 get the highest annual profit. They are compared and shown in Fig. 18(c).

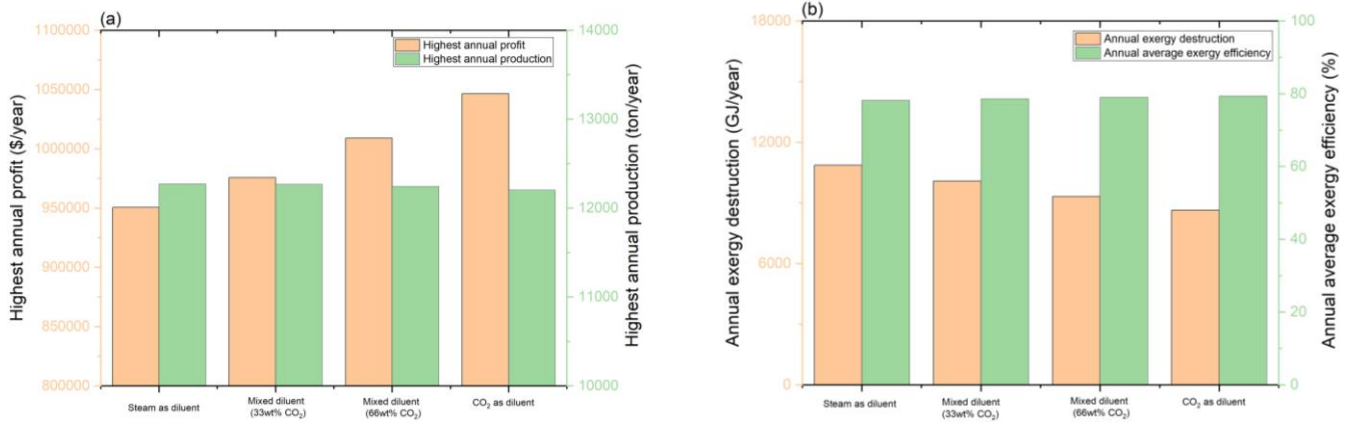


**Fig. 19.** Comparison of (a) highest annual production and highest annual profit (b) annual exergy destruction and annual average exergy efficiency when operating at the diluent-to-propane ratio with highest annual profit of PFR of 4 different scenarios

It can be observed from Fig. 19(a) that higher mass fraction of CO<sub>2</sub> in diluent slightly decreases the highest annual production since the loss in propylene yield is compensated by the increase of ethylene yield and run length. If only the annual production of PFR is considered, higher mass fraction of steam in diluent is preferred. However, higher mass fraction of CO<sub>2</sub> in diluent can increase the run length of PFR and decrease the energy consumption and cost of diluent. As shown in Fig. 19(a), higher mass fraction of CO<sub>2</sub> in diluent is preferred if considering the annual profit. When the pure/mixed diluent in 4 different scenarios operating at the ratio achieving highest annual profit, the annual exergy destruction and annual average exergy efficiency are compared and presented in Fig. 19(b). As shown in Fig. 19(b), higher mass fraction of CO<sub>2</sub> in diluent can significantly reduce the annual exergy destruction and slightly increase the annual average exergy efficiency when operating at the ratio achieving highest annual profit. Pure CO<sub>2</sub> as diluent is suggested since it not only can increase the highest annual profit but also can decrease the annual exergy destruction and increase the annual average exergy efficiency when operating at the ratio achieving highest annual profit.

## 6. Conclusion

In this paper, a 1-D pseudo-dynamic model was developed to study the PFR in radiation section of thermal cracking furnace. The model was implemented in gPROMS ModelBuilder® and validated using

1 industrial data from literature. The simulation results have shown good agreement with industrial data  
2 both under clean tube condition and at 700-hours run length. The model was then used to carry out  
3 process analysis of the economic and thermodynamic performance of PFR including: (1) impact of  
4 diluent-to-propane ratio using steam as diluent; (2) impact of diluent-to-propane ratio using CO<sub>2</sub> and  
5 compared with using steam; (3) comparison of pure/mixed diluents in 4 different scenarios. The key  
6 findings are: (1) When using steam as diluent, higher steam-to-propane ratio can increase the valuable  
7 products yields and run length of PFR while reduce the outlet flow rate of valuable products. PFR can  
8 reach the highest annual production at the steam-to-propane ratio 0.2 and reach the highest annual profit  
9 at the ratio 0.3. (2) When comparing CO<sub>2</sub> with steam as diluents, annual productions are similar, but the  
10 annual profit can be significantly increased because of longer run length and lower energy consumption.  
11 The highest annual profit can increase by 10.10% when using CO<sub>2</sub> as diluent. When operating at the  
12 diluent-to-propane ratio achieving highest annual profit, using CO<sub>2</sub> as diluent can save 17.44% energy  
13 and reduce the exergy destruction by 20.53%. (3) When comparing the pure/mixed diluents in 4 different  
14 scenarios, pure CO<sub>2</sub> is suggested as diluent with highest annual profit and similar annual production. In  
15 addition, when operating at the diluent-to-propane ratio achieving highest annual profit, using pure CO<sub>2</sub>  
16 can increase the exergy efficiency and decrease the exergy destruction of PFR. These key findings  
17 provide significant operational guidance for existing cracking furnace using steam as diluent and provide  
18 insights for future new generation diluents design to reduce the energy demand and increase the annual  
19 profit of thermal cracking furnace for ethylene manufacturing. In addition, use CO<sub>2</sub> as diluent can promote  
20 the commercial deployment of carbon capture process for ethylene manufacturing since the extra cost of  
21 CO<sub>2</sub> transport and storage can be avoided. Carbon capture and in situ utilization for ethylene  
22 manufacturing can significantly reduce global CO<sub>2</sub> emissions released to atmosphere and mitigate  
23 climate change Further studies can focus on developing a more detailed model with carbon capture for  
24 ethylene manufacturing and in situ utilization since this study has the emphasis on the comparison of  
25 different diluents.

## Credit authorship contribution statement

**Yao Zhang:** Conceptualization, Methodology, Software, Validation, Writing – original draft, Writing – review & editing. **Hui Yan:** Writing – review & editing. **Daotong Chong:** Supervision, Funding acquisition. **Cailing Guo:** Writing – review & editing **Shengyuan Huang:** Software, Writing – review & editing. **Joan Cordiner:** Supervision, Writing – review & editing **Meihong Wang:** Conceptualization, Supervision, Funding acquisition, Writing – review & editing.

## Acknowledgement

The authors would like to acknowledge the financial support of the National Key Research and Development Program of China (Grant Number 2021YFE0112800) and EU RISE project OPTIMAL (Ref 101007963).

## References

- [1] Mohammad Fakhroleslam, and Seyed Mojtaba Sadrameli. "Thermal cracking of hydrocarbons for the production of light olefins; A review on optimal process design, operation, and control." *Industrial & Engineering Chemistry Research* 59, no. 27 (2020): 12288-12303. <https://doi.org/10.1021/acs.iecr.0c00923>.
- [2] Zhencheng Ye, Xiao Han, Guihua Hu, and Liang Zhao. "Comparative Life Cycle Environmental, Exergteic, and Economic Assessment of Three Hydrocarbon-Based Ethylene Production Routes." *Fuel* 333 (2023): 126359. <https://doi.org/10.1016/j.fuel.2022.126359>.
- [3] Cheng Zheng, Xiao Wu, and Xianhao Chen. "Low-Carbon Transformation of Ethylene Production System through Deployment of Carbon Capture, Utilization, Storage and Renewable Energy Technologies." *Journal of Cleaner Production* 413 (2023): 137475. <https://doi.org/10.1016/j.jclepro.2023.137475>.
- [4] Benfeng Yuan, Yu Zhang, Wenli Du, Meihong Wang, and Feng Qian. "Assessment of energy saving potential of an industrial ethylene cracking furnace using advanced exergy analysis." *Applied Energy* 254 (2019): 113583. <https://doi.org/10.1016/j.apenergy.2019.113583>.

- 1 [5] G-Y.Gao, M. Wang, C. Ramshaw, X-G. Li, and H. Yeung. "Optimal operation of tubular reactors for naphtha  
2 cracking by numerical simulation." *Asia-Pacific Journal of Chemical Engineering* 4, no. 6 (2009): 885-892.  
3 <https://doi.org/10.1002/apj.351>.
- 4 [6] Mohammad Shahrokhi, and Ali Nejati. "Optimal temperature control of a propane thermal cracking  
5 reactor." *Industrial & engineering chemistry research* 41, no. 25 (2002): 6572-6578.  
6 <https://doi.org/10.1021/ie0106783>.
- 7 [7] M. E. Masoumi, S. M. Sadrameli, J. Towfighi, and A. Niaei. "Simulation, optimization and control of a thermal  
8 cracking furnace." *Energy* 31, no. 4 (2006): 516-527. <https://doi.org/10.1016/j.energy.2005.04.005>.
- 9 [8] M. Berreni, and M. Wang, "Modelling and dynamic optimization of thermal cracking of propane for ethylene  
10 manufacturing." *Computers & chemical engineering* 35, no. 12 (2011): 2876-2885.  
11 <https://doi.org/10.1016/j.compchemeng.2011.05.010>.
- 12 [9] Mohammad Fakhroleslam, and Seyed Mojtaba Sadrameli. "Thermal/catalytic cracking of hydrocarbons for the  
13 production of olefins; a state-of-the-art review III: Process modeling and simulation." *Fuel* 252 (2019): 553-566.  
14 <https://doi.org/10.1016/j.fuel.2019.04.127>.
- 15 [10] S. M. Sadrameli "Thermal/catalytic cracking of hydrocarbons for the production of olefins: A state-of-the-art  
16 review I: Thermal cracking review." *Fuel* 140 (2015): 102-115.<https://doi.org/10.1016/j.fuel.2014.09.034>.
- 17 [11] MS Shokrollahi Yancheshmeh, S. Seifzadeh Haghighi, M. R. Gholipour, O. Dehghani, M. R. Rahimpour, and  
18 S. Raeissi. "Modeling of ethane pyrolysis process: A study on effects of steam and carbon dioxide on ethylene and  
19 hydrogen productions." *Chemical engineering journal* 215 (2013): 550-  
20 560.<https://doi.org/10.1016/j.cej.2012.10.078>.
- 21 [12] S. Seifzadeh Haghighi, M. R. Rahimpour, S. Raeissi, and O. J. C. E. J. Dehghani. "Investigation of ethylene  
22 production in naphtha thermal cracking plant in presence of steam and carbon dioxide." *Chemical Engineering*  
23 *Journal* 228 (2013): 1158-1167.<https://doi.org/10.1016/j.cej.2013.05.048>.
- 24 [13] Guihua Hu, Xiaoxu Li, Xiaoyan Liu, Jun Hu, Olajide Otitoju, Meihong Wang, Wenli Du, Zhencheng Ye, Jian  
25 Long, and Feng Qian. "Techno-economic evaluation of post-combustion carbon capture based on chemical  
26 absorption for the thermal cracking furnace in ethylene manufacturing." *Fuel* 331 (2023):  
27 125604.<https://doi.org/10.1016/j.fuel.2022.125604>.
- 28 [14] Xiaobo Luo, Meihong Wang, Eni Oko, and Chima Okezue. "Simulation-based techno-economic evaluation for  
29 optimal design of CO<sub>2</sub> transport pipeline network." *Applied Energy* 132 (2014): 610-  
30 620.<https://doi.org/10.1016/j.apenergy.2014.07.063>.

- 1 [15] K. M. Sundaram, and G. F. Froment. "Kinetics of coke deposition in the thermal cracking of propane." *Chemical*  
2 *Engineering Science* 34, no. 5 (1979): 635-644. [https://doi.org/10.1016/0009-2509\(79\)85108-8](https://doi.org/10.1016/0009-2509(79)85108-8).
- 3 [16] Stephen K. Layokun, and David H. Slater. "Mechanism and kinetics of propane pyrolysis." *Industrial &*  
4 *Engineering Chemistry Process Design and Development* 18, no. 2 (1979): 232-236.
- 5 [17] K. M. Sundaram, and G. F. Froment. "Modeling of thermal cracking kinetics—I: Thermal cracking of ethane,  
6 propane and their mixtures." *Chemical Engineering Science* 32, no. 6 (1977): 601-608.  
7 [https://doi.org/10.1016/0009-2509\(77\)80225-X](https://doi.org/10.1016/0009-2509(77)80225-X).
- 8 [18] K. Keyvanloo, J. Towfighi, S.M. Sadrameli, and A. Mohamadalizadeh. "Investigating the effect of key factors,  
9 their interactions and optimization of naphtha steam cracking by statistical design of experiments." *Journal of*  
10 *Analytical and Applied Pyrolysis* 87, no. 2 (2010): 224–30. <https://doi.org/10.1016/j.jaap.2009.12.007>.
- 11 [19] Yongli Wang, Feifei Huang, Siyi Tao, Yang Ma, Yuze Ma, Lin Liu, and Fugui Dong. "Multi-Objective Planning  
12 of Regional Integrated Energy System Aiming at Exergy Efficiency and Economy." *Applied Energy* 306 (2022):  
13 118120. <https://doi.org/10.1016/j.apenergy.2021.118120>.
- 14 [20] Mostafa Alizadeh and Seyed Mojtaba Sadrameli. "Modeling of Thermal Cracking Furnaces Via Exergy Analysis  
15 Using Hybrid Artificial Neural Network–Genetic Algorithm." *Journal of Heat Transfer-transactions of The Asme* 138  
16 (2016): 042801. DOI:10.1115/1.4032171.
- 17 [21] Feifei Shen, Meihong Wang, Lingxiang Huang, and Feng Qian. "Exergy analysis and multi-objective  
18 optimisation for energy system: a case study of a separation process in ethylene manufacturing." *Journal of*  
19 *Industrial and Engineering Chemistry* 93 (2021): 394 – 406. <https://doi.org/10.1016/j.jiec.2020.10.018>.
- 20 [22] Mortaza Aghbashlo, Hajar Rastegari, Hassan S. Ghaziaskar, Homa Hosseinzadeh-Bandbafha, Mohammad  
21 Hossein Nadian, Alireza Shafizadeh, Su Shiung Lam, and Meisam Tabatabaei. "Exergy, Economic, and  
22 Environmental Assessment of Ethanol Dehydration to Diesel Fuel Additive Diethyl Ether." *Fuel* 308 (2022): 121918.  
23 <https://doi.org/10.1016/j.fuel.2021.121918>.
- 24 [23] Peiye Zhang, Ming Liu, Yongliang Zhao, and Junjie Yan. "Performance analysis on the parabolic trough solar  
25 receiver-reactor of methanol decomposition reaction under off-design conditions and during dynamic processes."  
26 *Renewable Energy* 205 (2023): 583–97. <https://doi.org/10.1016/j.renene.2023.01.097>.
- 27 [24] Choe, Changwon, Junaid Haider, and Hankwon Lim. "Carbon Capture and Liquefaction from Methane Steam  
28 Reforming Unit: 4E's Analysis (Energy, Exergy, Economic, and Environmental)." *Applied Energy* 332 (2023):  
29 120545. <https://doi.org/10.1016/j.apenergy.2022.120545>.

- 1 [25] S. Kajitani, S. Hara, and H. Matsuda, "Gasification rate analysis of coal char with a pressurized drop tube  
2 furnace." *Fuel*, 81 (2002) 539-546. [https://doi.org/10.1016/S0016-2361\(01\)00149-1](https://doi.org/10.1016/S0016-2361(01)00149-1).
- 3 [26] B. Stanmore, and S. Visona, "The contribution to char burnout from gasification by H<sub>2</sub>O and CO<sub>2</sub> during  
4 pulverized-coal flame combustion." *Combustion and Flame*, 113 (1998). [https://doi.org/10.1016/S0010-  
5 2180\(97\)00166-1](https://doi.org/10.1016/S0010-2180(97)00166-1).
- 6 [27] D. Roberts, and D. Harris, "Char gasification in mixtures of CO<sub>2</sub> and H<sub>2</sub>O: Competition and inhibition." *Fuel*, 86  
7 (2007) 2672-2678. <https://doi.org/10.1016/j.fuel.2007.03.019>.
- 8 [28] H.-J. Mühlen, K.H. van Heek, and H. Jüntgen, "Kinetic studies of steam gasification of char in the presence of  
9 H<sub>2</sub>, CO<sub>2</sub> and CO." *Fuel*, 64 (1985) 944-949. [https://doi.org/10.1016/0016-2361\(85\)90149-8](https://doi.org/10.1016/0016-2361(85)90149-8).
- 10 [29] Karim, G. A., and D. Mohindra, "A Kinetic Investigation of the Water-Gas Shift Reaction in Homogeneous  
11 Systems", *J. Inst. Fuel*, **219** (1974).
- 12 [30] Nan ZHANG, Tong QIU, and Bingzhen CHEN. "CFD Simulation of Propane Cracking Tube Using Detailed  
13 Radical Kinetic Mechanism." *Chinese Journal of Chemical Engineering* 21, no. 12 (2013): 1319–31.  
14 [https://doi.org/10.1016/s1004-9541\(13\)60619-9](https://doi.org/10.1016/s1004-9541(13)60619-9).
- 15 [31] Guihua, Hu, Honggang Wang, and Feng Qian. "Numerical Simulation on Flow, Combustion and Heat Transfer  
16 of Ethylene Cracking Furnaces." *Chemical Engineering Science* 66, no. 8 (2011): 1600–1611.  
17 <https://doi.org/10.1016/j.ces.2010.12.028>.
- 18 [32] Rezaeimanesh, Mohsen, Ali Asghar Ghoreyshi, S.M. Peyghambarzadeh, and Seyed Hassan Hashemabadi.  
19 "A Coupled CFD Simulation Approach for Investigating the Pyrolysis Process in Industrial Naphtha Thermal  
20 Cracking Furnaces." *Chinese Journal of Chemical Engineering* 44 (2022): 528–42.  
21 <https://doi.org/10.1016/j.cjche.2021.03.028>.
- 22 [33] José O. "Valderrama. Cubic equations of State." *Phase Behavior of Petroleum Reservoir Fluids* (2006):77–  
23 94. doi:10.1201/9781420018257-7.
- 24 [34] ABBOTT MM. "Cubic equations of state: An interpretive review." *Advances in Chemistry* (1979):47–70.  
25 doi:10.1021/ba-1979-0182.ch003.
- 26 [35] Lopez-Echeverry JS, Reif-Acherman S, Araujo-Lopez E. "Peng-Robinson Equation of State: 40 years through  
27 Cubics." *Fluid Phase Equilibria* (2017); 447:39–71. doi:10.1016/j.fluid.2017.05.007.
- 28 [36] P. Van Damme, S. Narayanan, and G. Froment, "Thermal cracking of propane and propane - propylene  
29 mixtures: Pilot plant versus industrial data." *AIChE Journal*, 21 (1975) 1065-1073.  
30 <https://doi.org/10.1002/aic.690210604>.

- 1 [37] Jan Szargut, David R. Morris, and Frank R. Steward. Exergy analysis of thermal, chemical, and Metallurgical  
2 Processes. New York: Hemisphere Publishing Corporation, 1988.
- 3 [38] R. Rivero, and M. Garfias. "Standard Chemical Exergy of Elements Updated." *Energy* 31, no. 15 (2006): 3310–  
4 26. <https://doi.org/10.1016/j.energy.2006.03.020>.
- 5 [39] Ali Ghannadzadeh, Raphaële Thery-Hetreux, Olivier Baudouin, Philippe Baudet, Pascal Floquet, and Xavier  
6 Joulia. "General Methodology for Exergy Balance in Prosimplus® Process Simulator." *Energy* 44, no. 1 (2012): 38–  
7 59. <https://doi.org/10.1016/j.energy.2012.02.017>.